Bechtel Nevada

REMOTE SENSING LABORATORY

DOE/NV/11718-127
UC-702

AERIAL RADIOLOGICAL SURVEYS

Alan E. Proctor

June 9, 1997

DISCLAIMER

June 9, 1997

DOE/NV/11718-127
UC 702

AERIAL RADIOLOGICAL SURVEYS

A. E. Proctor
Bechtel Nevada
Remote Sensing Laboratory
P.O. Box 98521
Las Vegas, Nevada 89193-8521
Telephone: (702) 295-8764 E-mail: proctoae@nv.doe.gov

ABSTRACT

Measuring terrestrial gamma radiation from airborne platforms has proved to be a useful method for characterizing radiation levels over large areas. Over 300 aerial radiological surveys have been carried out over the past 25 years including U.S. Department of Energy (DOE) sites, commercial nuclear power plants, Formerly Utilized Sites Remedial Action Program/Uranium Mine Tailing Remedial Action Program (FUSRAP/UMTRAP) sites, nuclear weapons test sites, contaminated industrial areas, and nuclear accident sites. This paper describes the aerial measurement technology currently in use by the Remote Sensing Laboratory (RSL) for routine environmental surveys and emergency response activities. Equipment, data-collection and -analysis methods, and examples of survey results are described.

1.0 INTRODUCTION

Aerial radiological survey methodology has been developed over the past 30 years. Initially developed by the RSL to respond to radiological emergencies related to the DOE's nuclear weapons program, the aerial survey capability has been expanded to include numerous routine and emergency response activities.

The purpose of an aerial radiation survey is to map the spatial distribution and concentration of gamma-emitting radionuclides. Real-life applications of this technique include (a) tracking and making initial assessments of radioactive plumes; (b) quickly and cost-effectively performing an overview of large, possibly contaminated areas; (c) examining populated or inaccessible areas that cannot be surveyed from the ground; and (d) providing assurance that man-made changes have not occurred in areas surrounding nuclear power plants and facilities that process radioactive materials. Over 300 aerial surveys have been carried out to date including DOE facilities, former nuclear weapons test sites, remedial action sites, nuclear power plants, industrial areas where radioactive materials were processed, several nuclear accident sites, the Kennedy Space Center, and the former USSR nuclear submarine training center. Many of these areas were known to be radioactively contaminated; others were surveyed to verify that contamination was present.

2.0 SURVEY METHODS

The RSL has developed aerial radiation surveying techniques for large-area gamma radiation surveys since the late 1960s. Earlier versions of this methodology have been reviewed in published reports.[1,2] Aerial gamma surveys are carried out using both fixed-wing and helicopter aircraft depending on the size of the survey area, the required degree of detail, and the survey costs. Figures 1 and 2 show the survey aircraft that are currently used. Rectangular detector "pods" mounted on the helicopter skids are visible in Figure 2.

2.1 Detector Characteristics

The detector system was designed to sense terrestrial and airborne gamma radiation having energies between 20 and 4,000 keV. This energy range includes emitted gamma radiation from naturally occurring radionuclides and almost all man-made gamma radiation sources. The sodium iodide, thallium-activated, NaI(T*l*), detectors are characterized by their variable sensitivity versus incident gamma energy and by a footprint size that is also energy-dependent. The variation in sensitivity with incident energy is a well-known characteristic of NaI(T*l*) detectors.

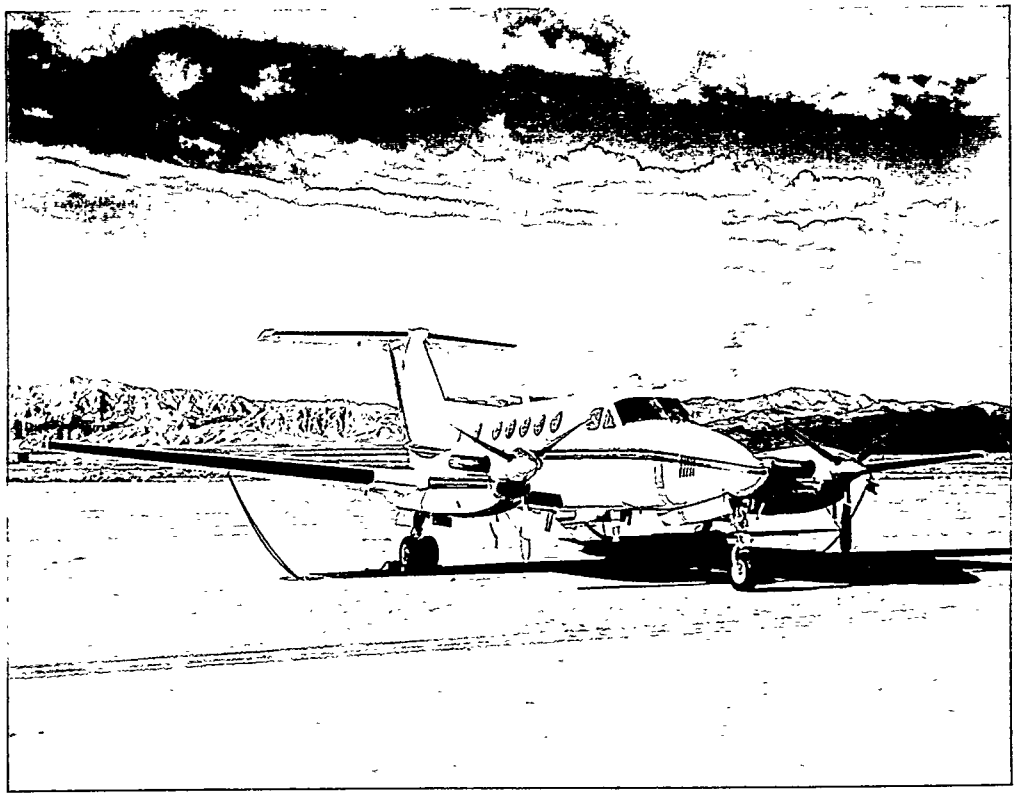

FIGURE 1. *FIXED-WING AIRCRAFT USED IN AERIAL RADIOLOGICAL SURVEYS*

Detailed data on detector sensitivity can be obtained from the manufacturer.[3] The dependence of the viewed footprint size with energy can be (approximately) modeled using methods described in Appendix A. Because of the large footprint, sources detected by aerial systems appear to be spread over a much larger area than would be indicated by ground-based measurements.

For uncollimated detectors such as those used in aerial surveys, the source-to-detector distance and the attenuation by the air effectively limit the viewed terrestrial area to a circular region centered beneath the detector. The size of the field of view is a function of the gamma-ray energy, the gamma-ray origin, and the detector response. Radionuclide activities on or in the soil and exposure rates normalized to one meter above ground level (AGL) are customarily reported but only as large-area averages. Activity, inferred from aerial data, for a source uniformly distributed over a large area compared to the field of view of the detectors is very good and generally agrees with ground-based measurements. However, activity for a point source, a line source, or a source activity less than the detector's field of view will be underestimated, sometimes by orders of magnitude. When this occurs, the aerial data simply serve to locate and identify such sources.

Apparent source-broadening makes comparison with ground-based measurements difficult. Radionuclides that occur as hot particles are averaged by the aerial detection system, appearing as uniform, large-area distributions. Ground surveys, however, would locate the hot particles within a smaller area and show the surrounding areas to be free of contamination. Table 1 contains estimates of the detection system's field of view or "footprint" size for several energies of interest.

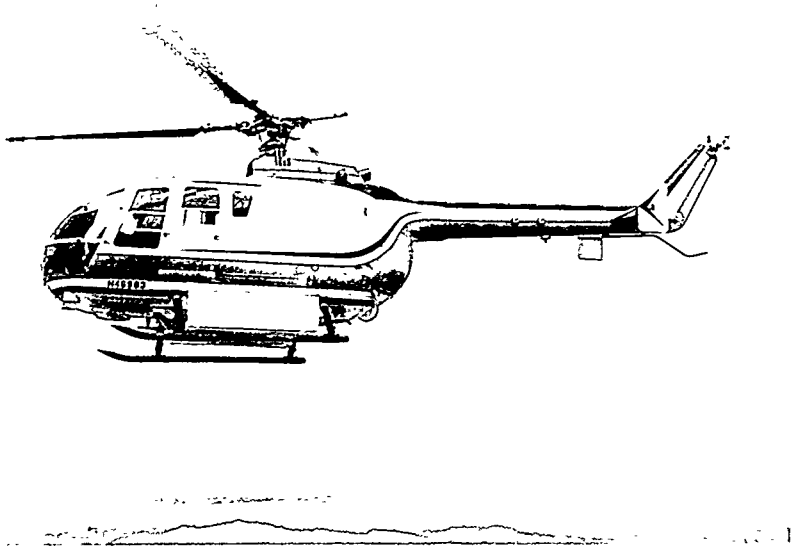

FIGURE 2. *HELICOPTER WITH DETECTOR PODS*

Table 1. Approximate Detector Footprint Radius for Relative Count-Rate Contributions from Terrestrial Sources at a Survey Altitude of 150 ft (46 m)

Emitted Gamma-Ray Energy (keV)	Radius Where 99% of the Detected Counts Originate (ft) (m)	Radius Where 90% of the Detected Counts Originate (ft) (m)	Radius Where 50% of the Detected Counts Originate (ft) (m)
60	650 (198)	353 (108)	155 (47)
200	850 (259)	435 (133)	178 (54)
600	1,067 (325)	560 (171)	214 (65)
1,500	1,715 (523)	772 (235)	260 (79)
2,000	2,145 (654)	850 (259)	275 (84)
3,000	2,862 (872)	1,007 (307)	308 (94)
4,000	3,850 (1173)	1,150 (351)	322 (98)
6,000	4,295 (1309)	1,325 (404)	350 (107)

Detector sensitivity is not constant throughout the footprint. The maximum sensitivity occurs directly beneath the detector; the sensitivity decreases with increasing horizontal distance between the source and airborne detector. Additionally, the incident gamma rays from even a monoenergetic source include scattered gamma rays once the incident radiation reaches the airborne detectors. Footprint sizes are, therefore, dependent on the source location: distributed in the soil, dispersed in the air, shielded inside a container, etc.

2.2 Collecting Radiation Data from the Aircraft

Data collection methods are similar for both aircraft platforms; Figure 3 illustrates important details of the aerial radiological surveying process. Gamma-ray spectral data are acquired by flying the helicopter platform along a series of uniformly spaced parallel lines at a fixed altitude (e.g., 150 ft [46 m] AGL). Data are acquired continuously along these lines and recorded in one-second intervals at an airspeed of 70 knots (36 m/s). This one-second interval corresponds to a 118-ft (36-m) data interval. Comparable survey parameters for fixed-wing aircraft include a 300–500 ft (91–52 m) altitude; line spacings of 500, 1,000, or 1,500 ft (152, 305, or 457 m); and airspeeds of 120–180 knots (62–93 m/s).

Two gamma-ray spectra are accumulated from eight NaI(T*l*) detectors during each one-second interval. Other information, such as air temperature, pressure, and altitude, is also recorded during each interval.

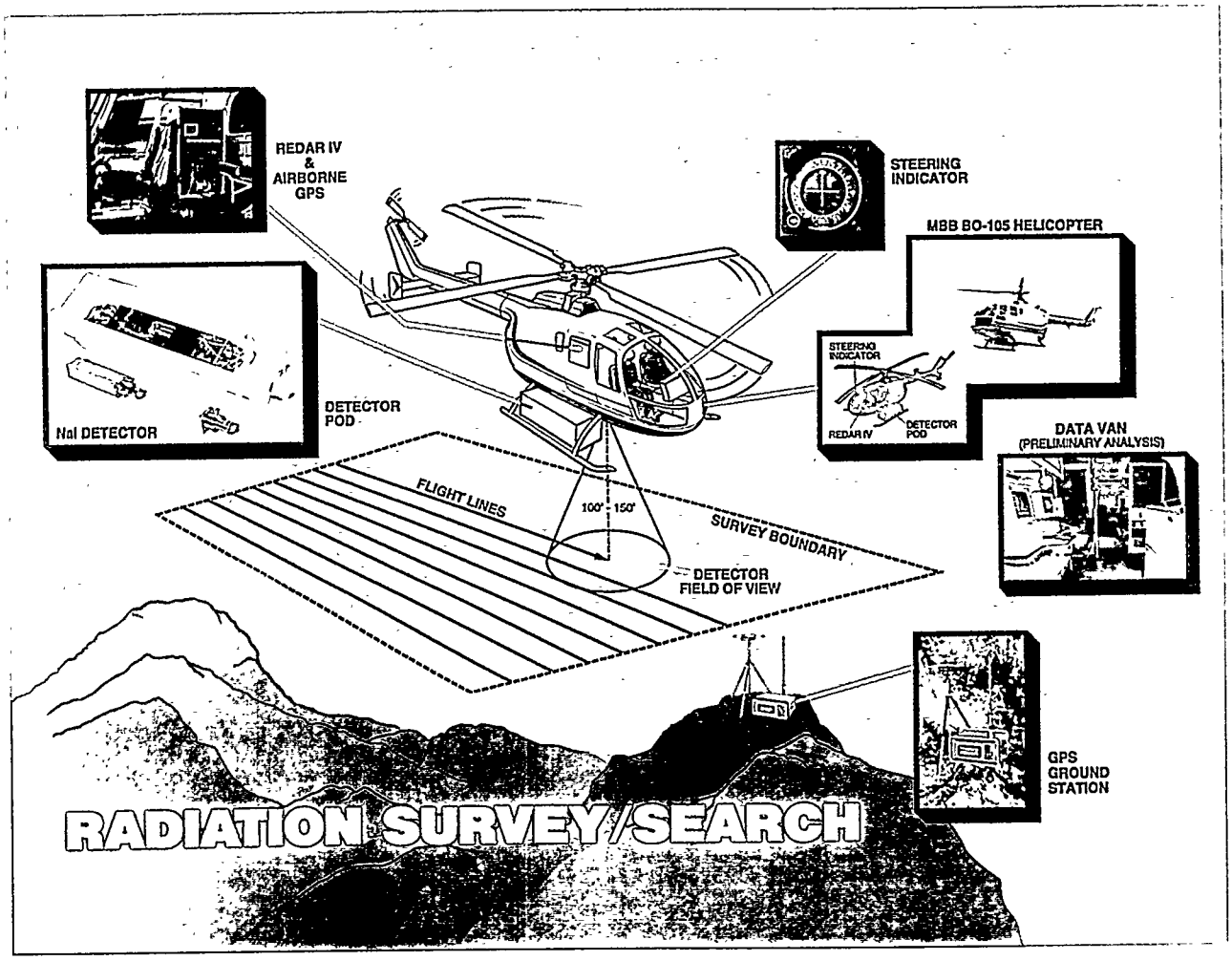

FIGURE 3. *AERIAL RADIOLOGICAL SURVEY OPERATIONS*

Aircraft position is established by a Global Positioning System (GPS) operated in differential mode. Real-time aircraft positions were determined by an on-board GPS receiver, based on the measured position from GPS satellite data and a correction transmitted from a second GPS station located at a known position on the ground. The airborne GPS receiver provides continuous positional data to a microprocessor that reformats the data for use in the RSL's airborne, computerized data-logging system. This on-board computer records the positional data and operates a steering indicator to aid the pilot in flying a set of equally spaced straight lines.

Real-time altitude measurements are made through a radar altimeter that measures the return time for a pulsed signal and converts this delay to aircraft altitude. For altitudes up to 2,000 ft (610 m), the manufacturer's stated accuracy is ±2 ft (0.6 m) or ±2 percent, whichever is greater. Altitude data were also recorded by the data-acquisition system so that variations in gamma signal strength caused by altitude fluctuations can be identified.

2.3 Data-Acquisition System

The helicopter detection system consists of eight 2- × 4- × 16-in downward-looking and two 2- × 4- × 4-in upward-looking NaI(T*l*) scintillation detectors installed in two rectangular aluminum pods. The fixed-wing survey aircraft carry from one to eight 2- × 4- × 16-in downward-looking and one 2- × 4- × 4-in upward-looking NaI(T*l*) scintillation detectors, depending on the survey application. Pulse inputs from the 2- × 4- × 16-in detectors are summed and recorded as a spectrum, as discussed below. In addition, a spectrum from one of the 2- × 4- × 16-in detectors is recorded separately to provide increased dynamic range when viewing higher-radiation areas. Counts from the 2- × 4- × 4-in detector are recorded for possible use in correcting nonterrestrial radiation contributions. The 2- × 4- × 16-in detectors are surrounded by thermal insulating foam and shielded on the top and sides with 0.03-in (0.076-cm) cadmium and lead sheets. The 2- × 4- × 4-in detectors are shielded on the bottom and sides with the cadmium and lead sheets.

Spectral data are acquired and displayed in real time using specialized instrumentation that processes, stores, and displays spectral data. This system was developed for aerial radiological surveys and contains the necessary instrumentation in a single package. The system, called the Radiation and Environmental Data Acquisition and Recorder, Version IV, (REDAR IV) system, is a multi-microprocessor and a portable data-acquisition and real-time analysis system.[4] It has been designed to operate in the severe environments associated with platforms such as helicopters, fixed-wing aircraft, and various ground-based vehicles. The system displays the required radiation and system information to the operator in real time. Pertinent data are recorded on cartridge tapes for later analysis.

The REDAR IV contains six subsystems: two independent systems to collect radiation data, a general purpose data input/output (I/O) system, a tape recording/playback system, a cathode-ray tube (CRT) display system, a real-time data-analysis system, and a ranging system having steering calculation and display capabilities. These subsystems, which are under the operator's control, handle functions including data collection, analysis, and display; positional and steering calculations; and

data recording. Two multichannel analyzers (MCAs) in the REDAR IV system collect 1,024-channel, gamma-ray spectra (4.0 keV per channel) once every second during the surveying operation. The primary MCA (for the eight-detector spectrum) has a usable dynamic range of approximately 100,000 cps corresponding to an exposure rate at one meter AGL of about 1.5 mR/h. Spectral information at high-count rates begins to degrade at approximately half this rate; a single NaI(T*l*) detector and second MCA are used when the system is used in high-count-rate situations.

The data-acquisition system is calibrated to a 0–4,000-keV energy range using gamma-ray sources of americium-241 (^{241}Am) at 60 keV, cobalt-60 (^{60}Co) at 1,173 and 1,332 keV, and cesium-137 (^{137}Cs) at 661 keV. A 28-keV, low-energy threshold is selected to minimize counts from the lower part of the continuum. The summed signals derived from each of the eight NaI(T*l*) detectors are adjusted prior to processing by the analog-to-digital converter so that the calibration peaks appeared in preselected channels in the MCA of the data-acquisition system.

Because the energy resolution of NaI(T*l*) crystals decreases with increasing energy, spectra are compressed to conserve storage space. Spectra are divided into three partitions where the detected photopeak width is approximately the same. Data in the first partition (0–300 keV) are not compressed to permit stripping of low-energy photopeaks such as the 60-keV photopeak from ^{241}Am. The second partition (300–1,620 keV) is compressed to 12 keV per channel while the third partition (1,620–4,000 keV) is compressed to 36 keV per channel. The highest channel contains all counts from gamma rays having energies greater than 4,000 keV.

Two full spectra, one spectrum containing data from the eight detectors and a second spectrum containing data from a single detector, and related information such as position, time, and air temperature are continuously recorded every second. The REDAR IV system has two sets of spectral memories; each memory can accumulate four individual spectra. The two memories support continuous data accumulation: one memory stores data while the other memory transfers data to magnetic tape. At a survey speed of 70 knots (36 m/s), 45 data sets are acquired for each mile of flight. A typical survey contains 40,000–60,000 data sets.

3.0 PRELIMINARY DATA ANALYSIS

Data processing is initiated in the field before leaving the survey site. Data are examined before leaving the site, and a preliminary analysis is completed to ensure that the raw data are satisfactory. Terrestrial exposure rates are computed from gross count data with a correction for variations in altitude. Man-made radioactivity and isotopic net count rates (e.g., ^{137}Cs, nitrogen-16 [^{16}N], and ^{60}Co) are determined through differences between total counts in appropriate spectral windows.

All count-rate data are smoothed using a three-point sliding interval average to reduce statistical fluctuations in the data:

$$C_{i,avg} = \frac{(C_{i-1} + C_i + C_{i-1})}{3}$$

$C_{i,avg}$ is the averaged value at the ith location, and C_{i-1}, C_i, and C_{i+1} are consecutive, corrected gross count rates along a single flight line. Present analysis codes do not average nearest-neighbor data on adjacent flight lines; three-point averaging has been found to be adequate. The exposure rate is calculated from this averaged gross count rate. Three-point sliding interval averaging was also applied to man-made and net isotopic data prior to calculating radiation contour maps. Two dimensional smoothing[5] is currently under investigation. Two-dimensional smoothing algorithms require regularly spaced data. Spacing between survey data positions follows flight lines and usually does not fall on an exact grid pattern. Smoothing may be applied to data that has been "binned" (i.e., averaged over a uniform grid).

3.1 Natural Background Radiation

Natural background radiation originates from radioactive elements present in the earth, airborne radon, and cosmic rays entering the earth's atmosphere. Natural terrestrial radiation levels depend on the types of soil and bedrock immediately below and surrounding the point of measurement. Within cities, the levels of natural terrestrial radiation also depend on the nature of the pavement and building materials. The gamma radiation originates primarily from the uranium and thorium decay chains and from radioactive potassium. Local concentrations of these nuclides produce radiation levels at the surface of the earth typically ranging from 1–15 μR/h. Some areas having high concentrations of uranium and/or thorium in the surface minerals exhibit even higher-radiation levels, especially in the western states.[6] The peaks shown in Table 2 were found in a typical natural background spectrum. Measurement of natural background during a survey is an important check on system operation. Figure 4 shows a typical spectrum from natural background radiation.

Isotopes of the noble gas radon are members of both the uranium and thorium radioactive decay chains. Radon can diffuse through the soil and may travel through the air to other locations. Therefore, the level of airborne radiation due to these radon isotopes and their daughter products at a specific location depends on a variety of factors including meteorological conditions, mineral content of the soil, and soil permeability. Typically, airborne radon contributes 1–10 percent of the natural background radiation.

Cosmic rays interact with elements of the earth's atmosphere and soil. These interactions produce an additional natural source of gamma radiation. Radiation levels due to cosmic rays vary with altitude and geomagnetic latitude. Typically, values range from 3.3 μR/h at sea level in Florida to 12 μR/h at an altitude of 1.9 mi (3 km) in Colorado.[7]

4.0 MEASURED TERRESTRIAL EXPOSURE AND MAN-MADE EXPOSURE RATES

Exposure rates are of interest for public health studies and post-accident decontamination efforts. The most basic of aerial radiological measurements, exposure rate at the aircraft is proportional to

Table 2. Gamma-Ray Photopeak Identifications—Background within a Typical Survey Area

Energy (keV)	Identification
240	^{208}Tl (239 keV), ^{228}Ac (209 keV), ^{212}Pb (238 keV)
380	^{228}Ac (339 keV), ^{214}Bi (387 keV, 389 keV)
511 (weak)	^{208}Tl (511 keV), annihilation
610	^{214}Bi (609 keV)
830 (weak)	^{228}Ac (795 keV), ^{208}Tl (861 keV)
930	^{228}Ac (911 keV), ^{214}Bi (934 keV)
1,130	^{214}Bi (1,120 keV)
1,230	^{214}Bi (1,238 keV)
1,460	^{40}K (1,460 keV)
1,750	^{214}Bi (1,765 keV)
2,160	^{214}Bi (2,204 keV)
2,560	^{208}Tl (2,614 keV)

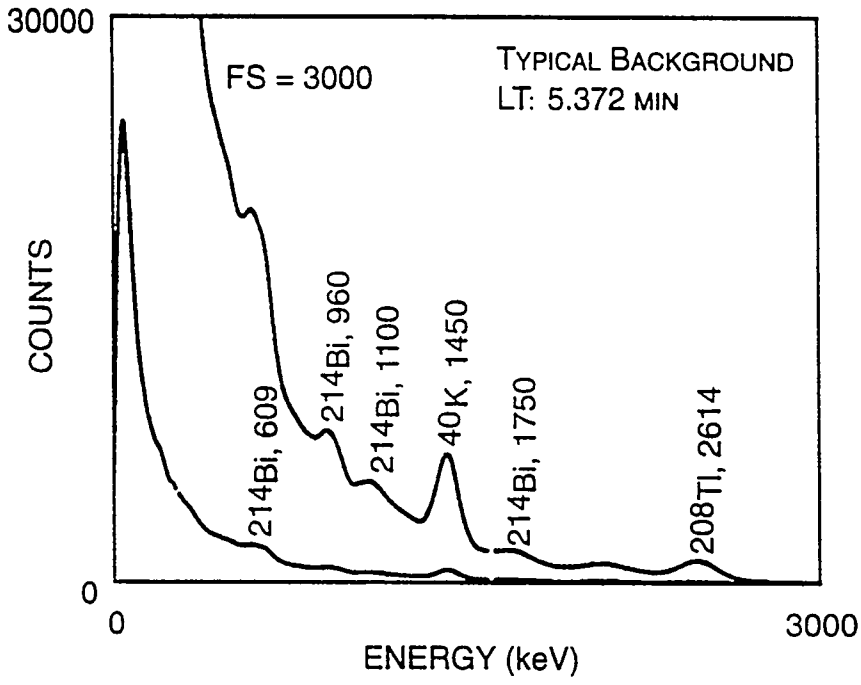

FIGURE 4. *GAMMA SPECTRUM OF A TYPICAL BACKGROUND AREA*

the detector gross count rate. The measured count rate in the aircraft differs from the true terrestrial exposure rate due to background sources in the aircraft, variations in cosmic radiation with altitude, temporal variations in atmospheric radon concentrations, and attenuation by the air of gamma rays emitted from the ground. Because raw count-rate data collected over a survey area have been found to vary, data from each flight are normalized to data that are measured over a test line at the beginning and end of each data-acquisition flight. This normalization is used to minimize the effects of variations in the natural airborne and background aircraft radiation.

The "actual" terrestrial exposure rate can be calculated as follows:

$$Exposure\ Rate = (Conversion\ Factor)\ (GC - B)\ e^{-(A \cdot altitude)}$$

GC is the gross count rate (sum of the contents of all spectrum channels) recorded by the REDAR IV system, and *A* and *B* are constants. *A* is the site-specific, atmospheric attenuation coefficient and has been found to be constant over the duration of a survey. *A* is determined from data taken at multiple altitudes over the test line. *B* represents the nonterrestrial background count rate and is calculated from test-line count rates measured before and after each survey data flight (using the previously determined value of *A*). An average value of *B*, the recorded altitude at each data interval, and the value of *A* are used to correct all measurements to yield the correct terrestrial gamma-emission rate. (Such a correction could be gamma-ray energy-dependent. At present, it is assumed that the relative contributions to the measured spectrum do not vary between the test line and the survey area, so an average correction is appropriate.)

The conversion factor, relating count rates to exposure rates, has been determined in several ways. It can be determined empirically by comparing ground-based, exposure-rate measurements of a well-characterized reference line with count rates from the airborne system. Two reference lines are maintained for survey calibration: one in Calvert County, Maryland, and a second in the Lake Mohave National Recreation Area near Las Vegas, Nevada. A conversion factor of 1.04×10^{-3} μR/h $(cps)^{-1}$ was recently determined using the Calvert County, Maryland, reference line.[8,9]

This conversion factor and exposure rates that were calculated using the conversion factor are correct only in regions of natural background radiation. Rates in regions where the gamma-ray spectrum is dominated by man-made activity are useful as relative indicators. For example, the spectrum near a boiling-water reactor plant site is significantly different from natural background due to the presence of gamma rays from ^{16}N.[10]

Terrestrial exposure-rate isopleth plots are also used as quality checks on the systematic variability of survey data. In particular, exposure-rate isopleths that fall along flight lines, especially along the initial or final lines of individual flights, indicate instability in the detection system. Such variations must be corrected before the data are used. If they cannot be corrected, the uncertainty (error bars) applied to the isopleth plots must be increased to eliminate obvious systematic variations.

4.1 Identifying Sources of Man-Made Radiation from Aerial Survey Data

Contaminated sites are located from isopleth maps based on a man-made radiation source algorithm, referred to as the man-made gross count rate (MMGC). This analysis provides a general overview of contamination within the survey area and also indicates the areas that should be further investigated. The MMGC algorithm is based on several observations: (a) commonly occurring man-made sources emit gamma rays having energies less than 1,394 keV while natural background sources emit gamma rays both below and above this threshold and (b) the spectrum continuum shape is relatively constant throughout the survey area. Moreover, gamma rays detected after they are scattered (*i.e.*, emitted by sources buried in soil or through atmospheric scattering) will contribute to the continuum at energies below their initial energies.

The measured spectral shape is constant over the survey area assuming a (a) stable cosmic-ray emission rate; (b) a constant background due to the aircraft, airborne radon, and natural sources; and (c) a survey area where the gamma sources and soil composition change slowly in relative comparison to the area contributing to the measured spectrum. Experience has shown that these assumptions are reasonable within statistical uncertainties over large, uncontaminated survey areas. (Significant changes in the source characteristics will invalidate this assumption. For example, changes in the MMGC are seen in spectra acquired over different terrain and when airborne radon levels change.)

If there were no systematic errors in the detection system, the sum of all gamma radiation due to man-made sources would be the difference between the spectrum in question and a typical background spectrum. Unfortunately, systematic errors make this simple subtraction impractical. A more reliable comparison can be made using the ratios of the sum of all channel contents of the spectral region from 38–1,394 keV (the region of man-made gamma emitters) to the sum of the spectral region from 1,394–3,026 keV (the region containing mostly counts from naturally occurring gamma emitters).

$$MMGC = \sum_{E=38\ keV}^{1394\ keV} C_i - \left(Normalization \cdot \sum_{E=1394\ keV}^{3026\ keV} C_i \right)$$

C_i represents the contents of spectrum channels corresponding to energies within the range of summation. The MMGC is the difference for a spectrum measured over an area containing man-made radionuclides, computed using the previously determined normalization constant. The constant is computed from data measured over areas free of contamination as follows:

$$Normalization\ \ Constant = \frac{\sum_{E \cdot 38\ keV}^{1394\ keV} C_i}{\sum_{E \cdot 1394\ keV}^{3026\ keV} C_i}$$

The normalization constant is derived from the data of each flight to minimize the effects of airborne radon-222 (^{222}Rn) and minor system characterization differences between flights.

Detectable high-energy gamma rays, such as the 6.13-MeV gamma ray emitted by ^{16}N, interfere with the MMGC computation: the contribution to the Compton continuum due to high-energy gamma rays contributes to the total spectrum over a broad range of energies below the photopeak. This contribution changes the spectral shape, invalidating the assumption used to calculate the normalization constant.

MMGC values are likely to have less favorable statistical uncertainties than net counts for individual radionuclides since the MMGC is based on a difference of two relatively large numbers. However, the MMGC is useful as a "first look" that can be used to determine if further isotopic analysis is warranted.

4.2 Rancho Seco Nuclear Power Plant

Two aerial radiological surveys were carried out at the Rancho Seco Nuclear Power Plant. The first survey, performed in 1980, established a baseline for exposure rate and man-made contamination in the area surrounding the site.[11] The second survey, performed in 1984, clearly showed the spread of contamination.[12]

Beginning in 1980, a U.S. Nuclear Regulatory Commission licensee began discharging a liquid radioactive effluent from the Rancho Seco station into nearby Clay Creek. By the summer of 1984, elevated contamination levels due to ^{134}Cs, ^{137}Cs, and ^{60}Co were found in several areas along the Clay, Hadselville, and Laguna Creeks.

The 1984 aerial survey was used to determine the extent of man-made contamination. The survey covered a 30-sq-mi (75-sq-km) area over the plant site and the drainage paths of the Clay, Hadselville, and Laguna Creeks. Figure 5 shows the exposure-rate contour map based on the 1984 survey data. Exposure-rate changes that occurred after the 1980 aerial survey are shown in blue. Except in the area surrounding the plant site, exposure rates were detected as expected for the area surrounding the plant site.

Large changes were seen in the MMGC levels between 1980 and 1984. Figure 6 shows the MMGC levels based on the 1980 survey data; Figure 7 shows the 1984 MMGC results. (The MMGC for both the 1980 and 1984 surveys were processed in the same way.) Evidence of the migration of contamination along the three creeks and their tributaries is readily visible. In addition, the migration path is only along the creek; no airborne deposition, for example, was present.

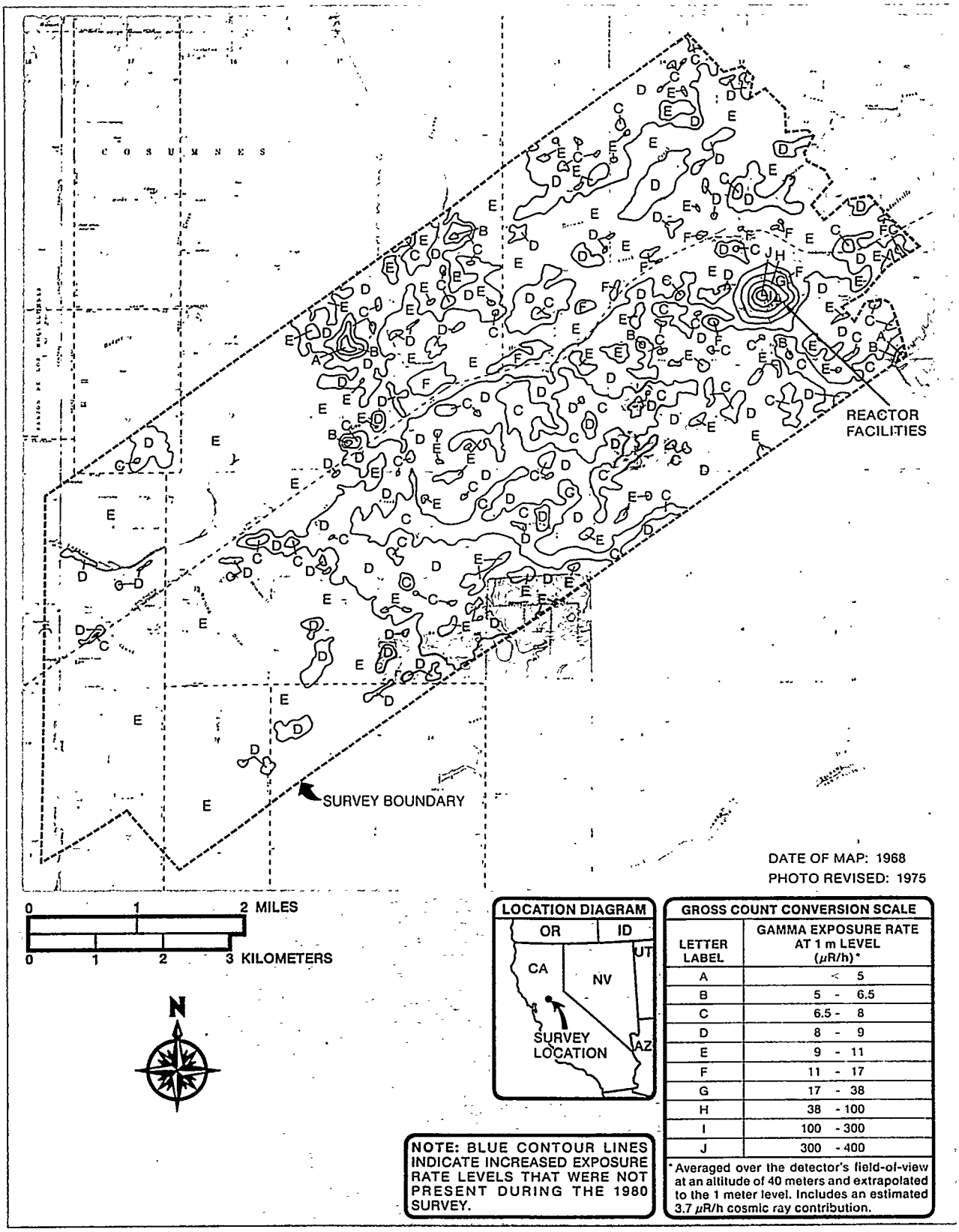

FIGURE 5. *RANCHO SECO EXPOSURE-RATE MAP*

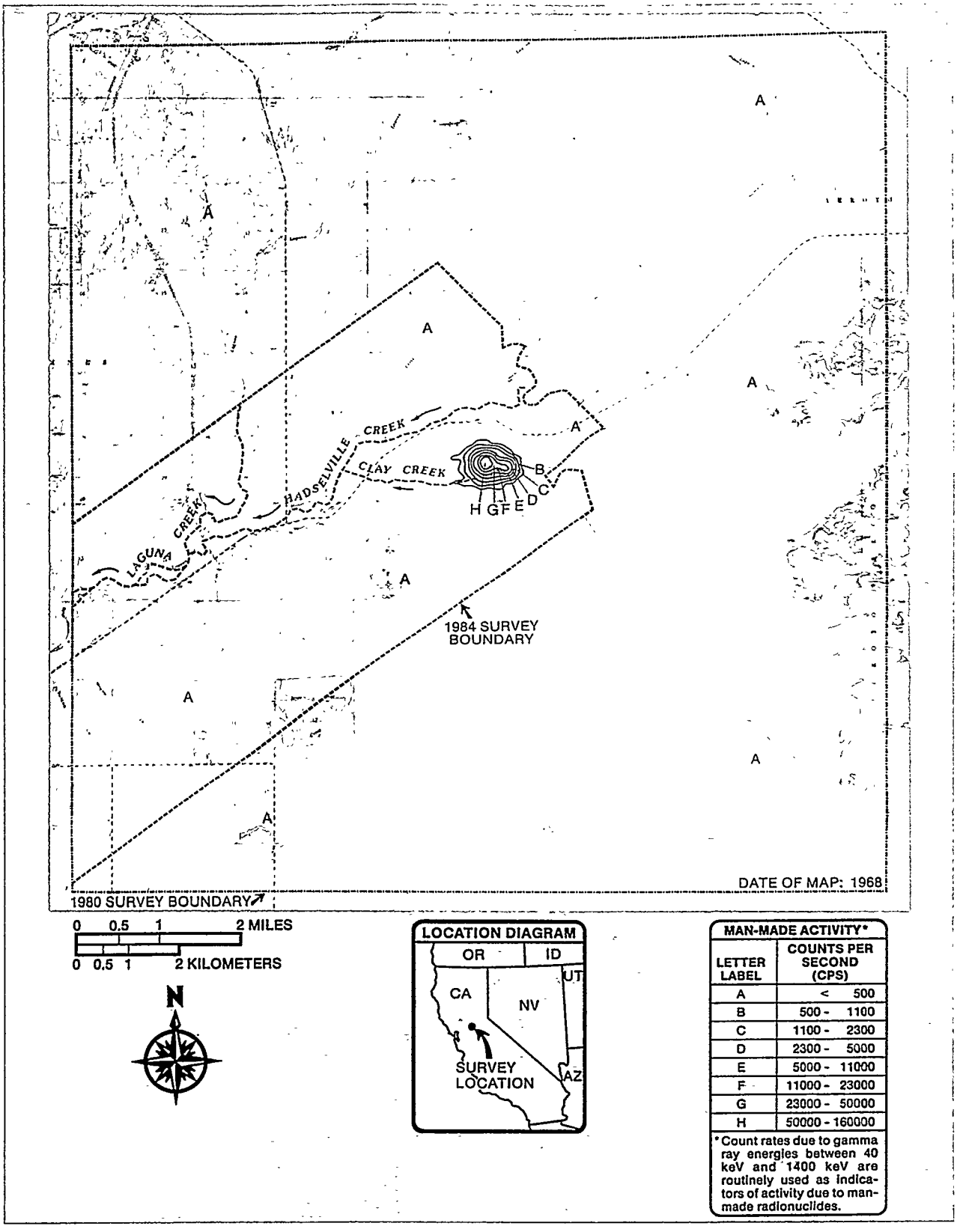

FIGURE 6. *RANCHO SECO 1980 MAN-MADE CONTAMINATION*

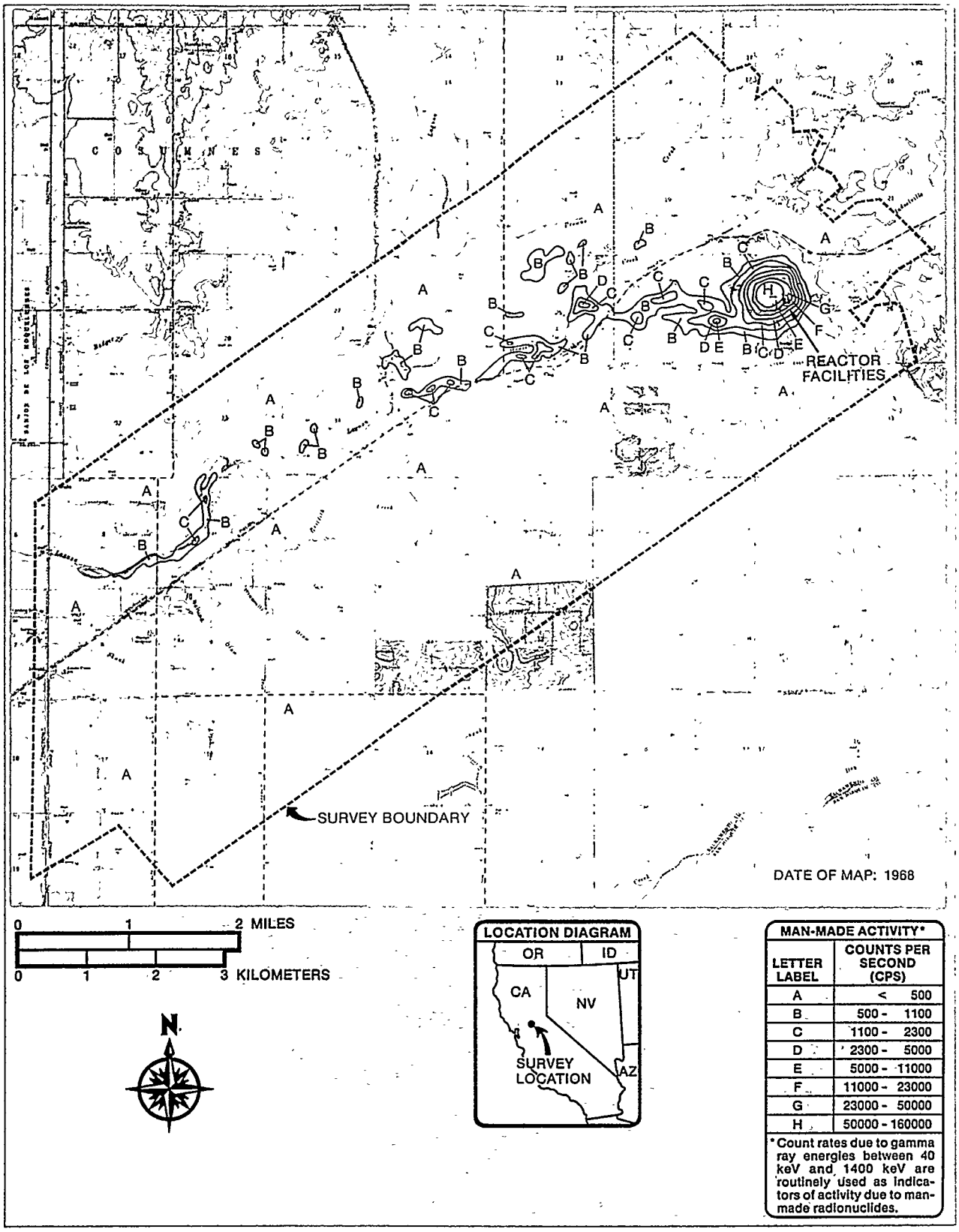

FIGURE 7. *RANCHO SECO 1984 MAN-MADE CONTAMINATION*

Examination of spectra collected over the areas of elevated MMGC rates verified that the contamination was primarily due to ^{137}Cs, with some areas also showing detectable concentrations of ^{134}Cs and ^{60}Co. Figure 8 is a spectrum collected over an area contaminated with these three radionuclides.

5.0 RADIONUCLIDE-SPECIFIC INFORMATION FROM AERIAL SURVEY DATA

While the MMGC provides an indication of radioactive contamination, positively identifying contamination sources is important for activities such as predicting risks to the public. Aerial survey data are summed and examined for spectral peaks due to various radionuclides that could reasonably be expected at the survey site. Annihilation radiation at 511 keV was also examined as this line was prominent in previous survey data from boiling-water reactor sites.

Spectral-stripping techniques were used to analyze aerial radiation data. (Peak fitting is not used because peak shapes from the NaI[T*l*] detectors are broad and frequently overlap.) Spectra from areas of interest (usually those with significant MMGC levels) are analyzed by subtracting, channel-by-channel, a spectrum of a known background area. These spectra are sums of all spectral data acquired within the area:

$$Difference\ Spectrum_i = C_{i,site\ of\ interest} - K_{diff} \cdot C_{i,background}$$

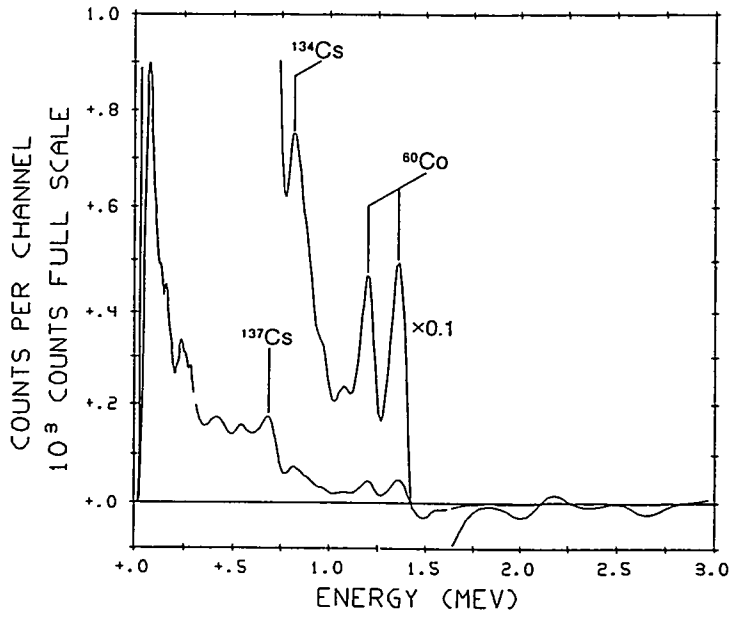

FIGURE 8. *RANCH SECO SPECTRUM FROM CONTAMINATED AREAS*

The K_{diff} constant is selected to force the difference spectrum to zero at the high-energy side. Spectral peaks are readily visible in the difference spectrum. The presence of an identifiable spectral peak is considered to be a requirement for proceeding with isotopic isopleth plots. Once identified, contour plots of individual radionuclides are computed using two- or three-window spectral-stripping techniques on each data spectrum acquired during the survey as follows:

$$Isotopic\ Net\ Count = \sum_{E=E_1}^{E_2} C(E) - (Scaling\ Factor) \cdot \left[\sum_{E=E_3}^{E_4} C(E) + \sum_{E=E_5}^{E_6} C(E) \right]$$

$C(E)$ represents the spectrum channel contents, and E_I represents the limiting energy ranges of the windows. This technique is shown graphically in Figure 9. Again, the scaling factor is adjusted to set the isotopic net count to zero for data from known background regions. This technique is similar to ordinary sample-counting practices, except that the "background" is established by using areas near the survey site rather than by using a "blank" sample. Net count uncertainties and estimated minimum detectable activities for isotopic analysis are discussed in Appendix B.

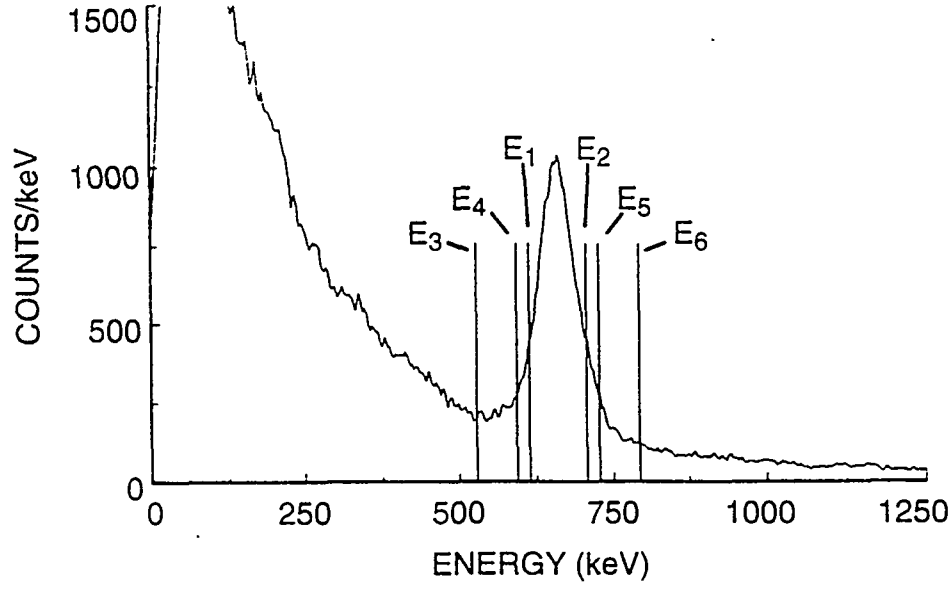

FIGURE 9. *SPECTRAL NET COUNT EXTRACTION*

5.1 Rocky Flats Plant Site

The Rocky Flats Plant produced plutonium-containing components for nuclear weapons. The plant was operated for the DOE by various contractors. By 1989, adverse publicity led to the establishment of a DOE "Tiger Team" that was mandated to determine if changes in the radiological conditions at the plant site and surrounding areas had occurred since a prior survey was conducted in 1981. There was interest in determining the possibility of off-site plutonium contamination and the possibility of accidental criticality events that may have occurred as a result of mishandling fissile plutonium.

The Rocky Flats Plant consists of manufacturing, chemical processing, laboratory, support, and storage facilities situated on a 255-acre (103-hectare) complex. The complex is situated in the center of a 6,550-acre (2650-hectare) natural preserve. The preserve is located 16 mi (27 km) north of Denver, Colorado, and is almost equidistant (10 m [16 km]) between the cities of Boulder and Golden. Developed areas adjoin the preserve.

An aerial survey was part of an effort to characterize the Rocky Flats site. Other work included *in situ* radiation measurements using high-resolution detectors and the counting of soil samples.[13] A survey area of 48 sq mi (124 sq km) was examined. This survey area included the plant site and sufficient area assumed to be without potential contamination to establish the local background levels.

Figure 10 shows the terrestrial exposure rates. Interesting features include the low levels over the lakes and a former uranium mine southwest of the plant site. No appreciable differences in exposure rate between the plant site and surrounding area were evident except for "hot spots" over several plant buildings. "Hot spots" over buildings known to contain nuclear materials were expected—note the broadening of the detected radioactivity due to the sizable detector "footprint."

The presence of plutonium contamination was investigated by measuring the ^{241}Am net count rate. Americium-241 is a daughter of ^{241}Pu, which is present in weapons-grade plutonium. Based on the expected ^{241}Pu concentration and an estimate of the age of the plutonium, contamination levels of plutonium would be 5–7 times the measured ^{241}Am levels. Figure 11 shows ^{241}Am over the plant site in a small area of the reservation. Based on calculated conversion factors, a 100-cps net ^{241}Am rate corresponds to a 18-pCi/g deposition (for a source exponentially distributed in the soil versus depth, relaxation length of 10 cm, and sampling depth of 10 cm). In terms of an equivalent surface distribution, the 100 cps corresponds to .0429 μCi/m^2. Conversion-factor derivation is discussed in Appendix A. This ^{241}Am level would correspond to 90–126 pCi/g (.22–.30 μCi/m^2) of plutonium. The minimum detectable activity for ^{241}Am was 11.2 pCi/g for a 5-cm depth sample. No plutonium contamination was found outside the preserve area.

The presence of ^{137}Cs, a common fission product, was considered an indicator of criticality accidents. Figure 12 shows the distribution of ^{137}Cs over a large area including the Rocky Flats preserve area. The 100 cps in Figure 12 correspond to a .092-μCi/m^2 surface deposition or a 1.2-pCi/g if the ^{137}Cs were uniformly distributed in the soil. These levels are comparable to those seen in this area due to

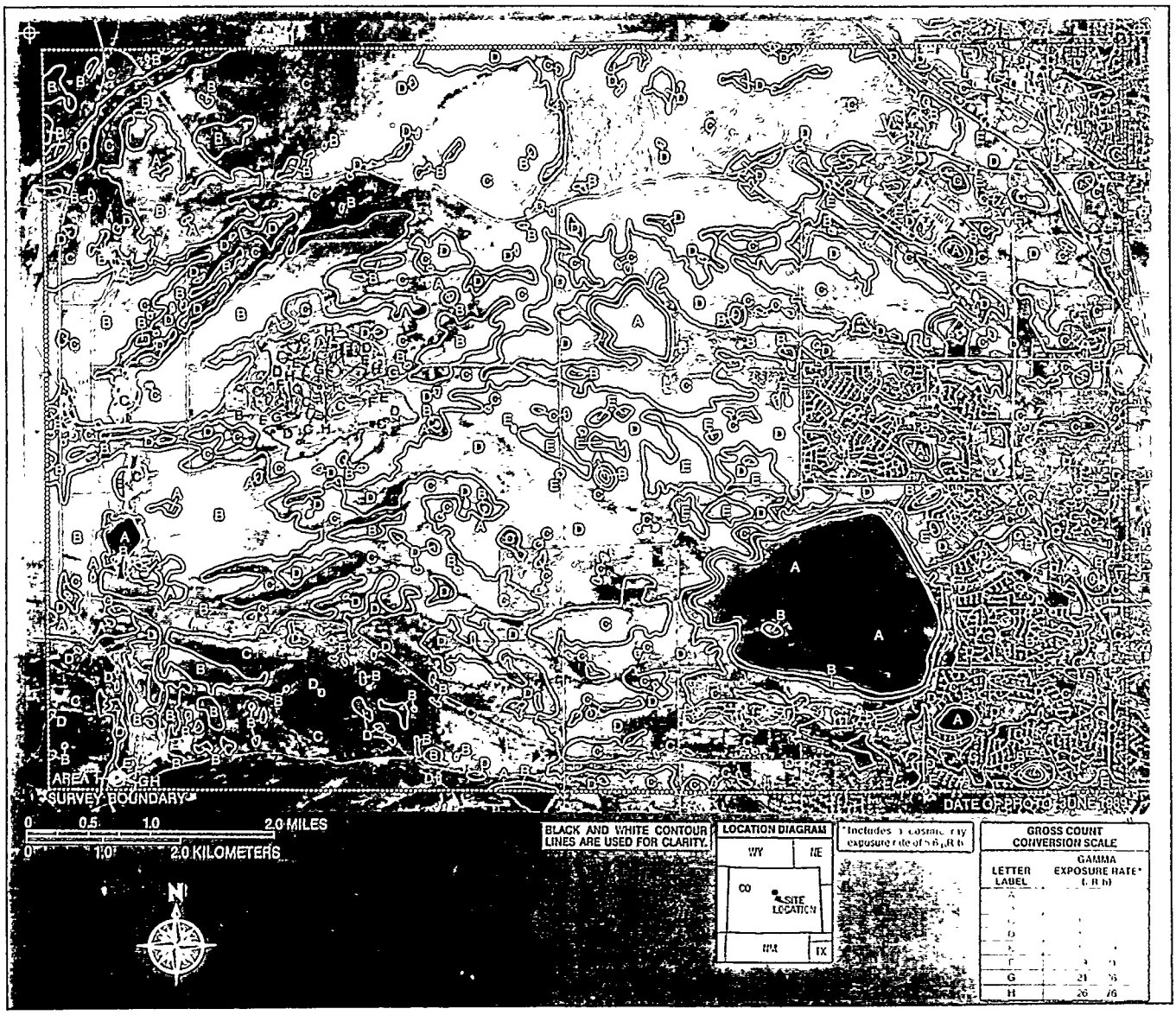

FIGURE 10. *ROCKY FLATS EXPOSURE-RATE MAP*

FIGURE 11. *ROCKY FLATS ^{241}Am MAP*

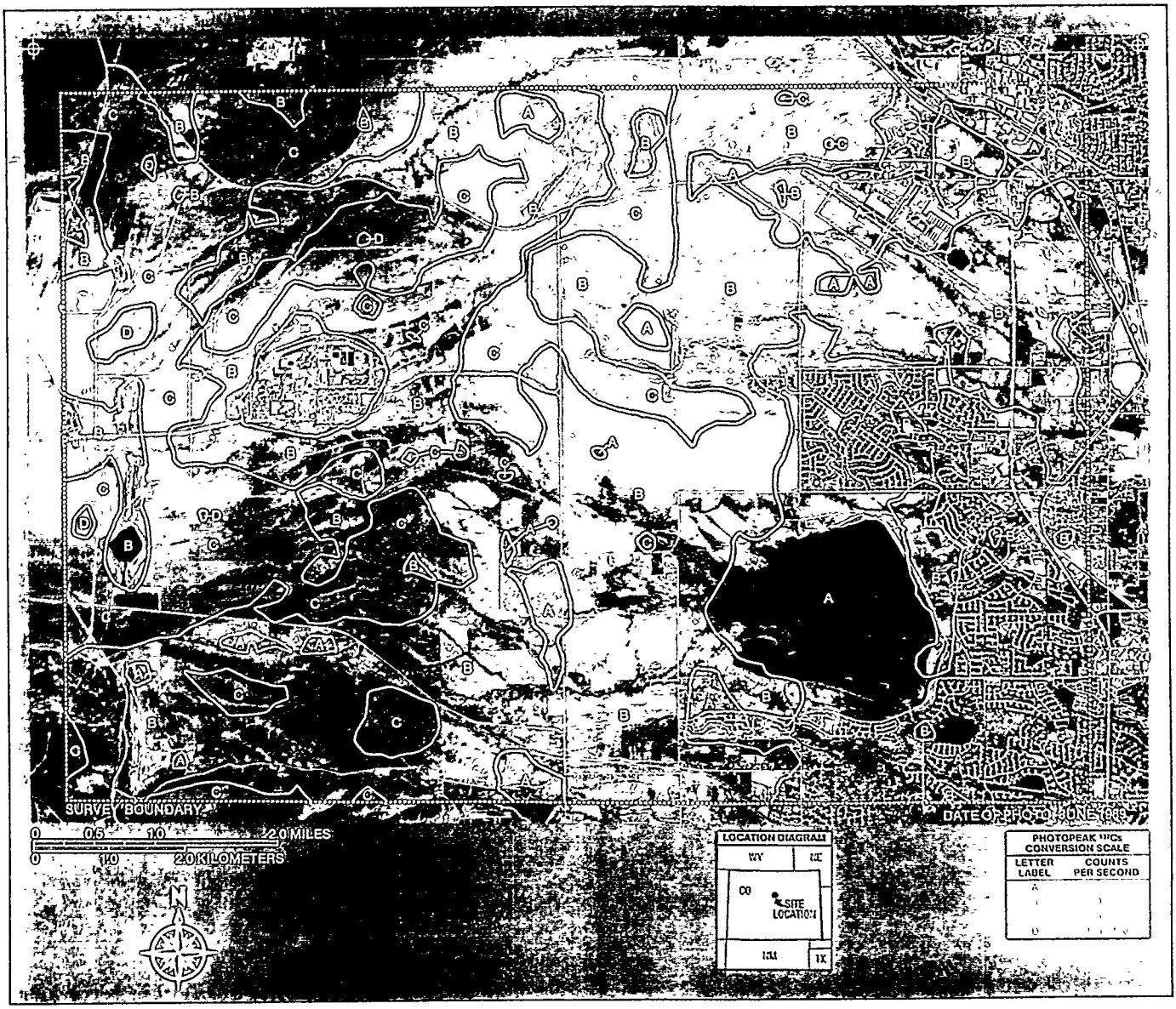

FIGURE 12. *ROCKY FLATS ^{137}Cs MAP*

worldwide fallout. Levels of ^{137}Cs can be seen to correlate with land development within the survey area. Housing tracts and the Rocky Flats plant site have lower ^{137}Cs levels than the surrounding undeveloped areas. This is an indication that these areas were developed after the end of atmospheric nuclear testing; grading the soil during development buried the ^{137}Cs fallout leading to lower-detection levels in the aerial survey. (It also indicated that the Rocky Flats plant did not release significant fission products during operation.)

5.2 Pocatello, Idaho

Phosphate fertilizer and elemental phosphorus are manufactured in Pocatello, Idaho, and nearby areas. Phosphate slag, a byproduct of these operations, was an economically attractive fill material. Unfortunately, normal processing of the phosphate ore concentrated naturally occurring uranium and thorium daughters in the slag. Extensive use of the slag resulted in exposure rates of two to three times higher than the "natural" background levels throughout the area. An aerial radiation survey was the method of choice to determine where the slag had been used within the developed urban area.

The presence of uranium and its daughters was sensed by detecting the "excess" uranium daughter, bismuth-214 (^{214}Bi).[14] Bismuth-214 emits a 1.76-MeV gamma ray. The net ^{214}Bi count rate was calculated by summing the aerial spectral data recorded between 1.58 and 1.93 MeV and subtracting a normalized sum of spectral background between 2.36 and 2.86 MeV. The normalization was chosen to force the net count rate to zero over uncontaminated areas, effectively removing contributions from naturally occurring radionuclides. Figure 13 shows the excess ^{214}Bi levels over the Pocatello airport and surrounding area. Radiation isopleths indicate the excess levels above natural background. Locations of paved roads and runway areas, where phosphate slag had been used, correlate nicely with elevated ^{214}Bi levels.

5.3 Double Tracks Site, Nellis Air Force Range, Central Nevada

The Double Tracks site is located on the Nellis Air Force Range, approximately 25 km (16 mi) east of Goldfield, Nevada, and 35 km (22 mi) southeast of Tonopah, Nevada, about 250 mi (420 km), from Las Vegas, Nevada. "Double Tracks" was an investigation of plutonium uptake by animals exposed to an explosive-driven (nonnuclear) airborne dispersal of nuclear weapons material. After completing the tests, the area was cleared of structures and the plutonium-contaminated area fenced. The site was left untouched until an aerial radiological survey of other sites from the same series of tests showed more extensive ^{241}Am contamination than anticipated. A new aerial radiological survey of the Double Tracks site was carried out in 1993[15] followed by a ground-based radiological survey using detectors mounted on a truck.[16] The two surveys provide a comparison between aerial and ground-based radiation measurements.

The Double Tracks aerial and ground surveys were incorporated into a plan to remove the contaminated soil from the site and return the site to unrestricted use. The aerial survey provided a broad view of the areas that would be of interest. The ground-based survey examined these areas, identifying locations that would require excavation. After excavating the contaminated material, a second ground-based survey provided assurance that contamination levels were below those required for unrestricted use.

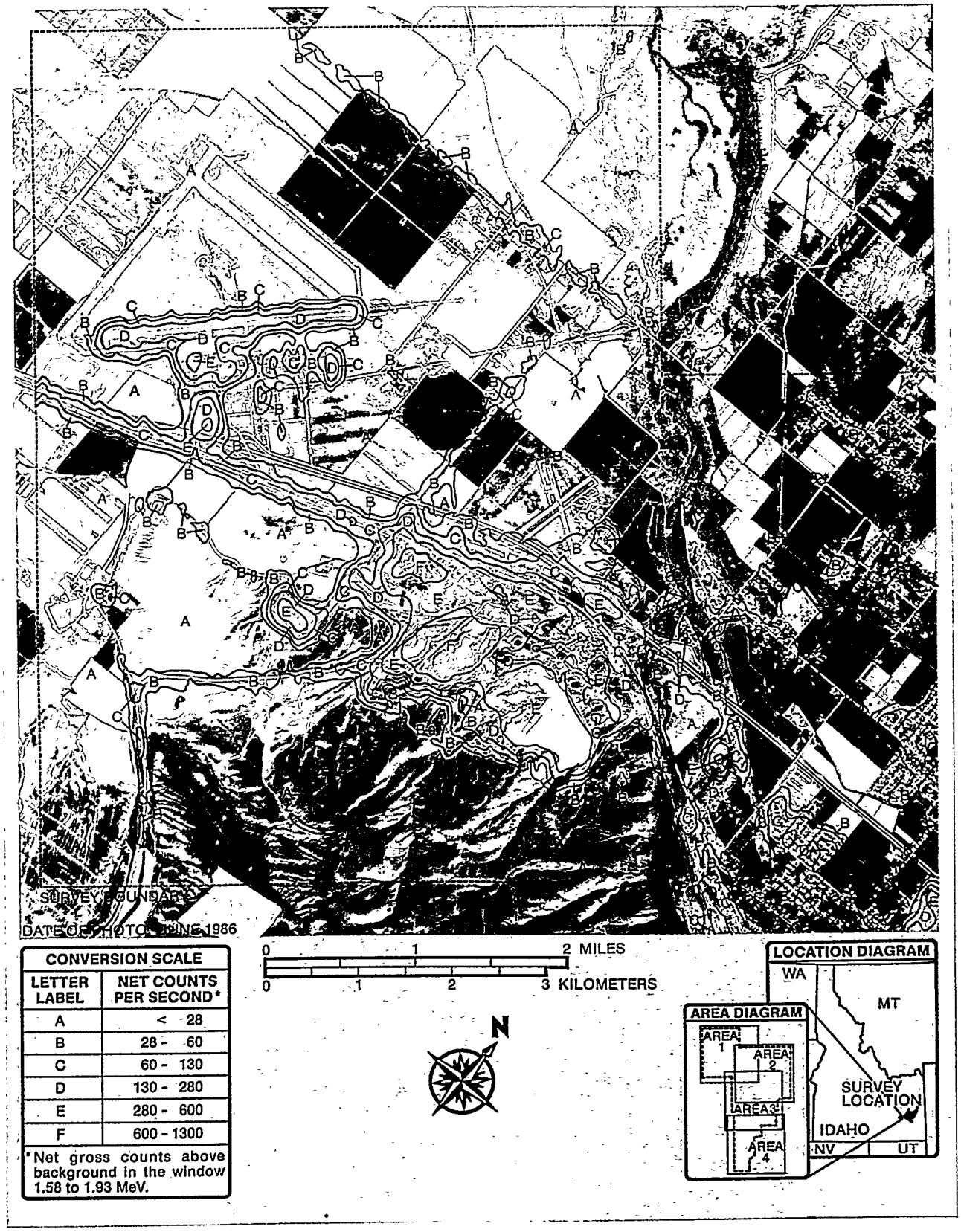

FIGURE 13. *EXCESS ^{214}Bi AT POCATELLO AIRPORT*

Figure 14 shows the plutonium levels at the Double Tracks site from the 1993 aerial survey. As with the Rocky Flats data, plutonium contamination levels were inferred from ^{241}Am. Measurable levels extended within the original fenced area. These data were later reprocessed by averaging groups of spectral data.[17] The area was divided into 150- × 150-ft and 450- × 450-ft squares. Survey data were separated by matching the data-point location with one of the mapped squares. All data falling into a particular square were averaged, creating a coarse resolution map of square "pixels"; the averaged spectra represented an averaged radiological environment in each square. For example, a 450- × 450-ft square contained data from 11 original survey spectra. Averaging in this way improved the minimum detectable activity. The results of this averaging are shown in Figure 15. Measurable plutonium is now evident beyond the fenced area. Spatial resolution near the "ground zero" location of highest contamination has been degraded.

Figure 16 shows the corresponding ground-based measurements. The detection system used in the ground-based survey viewed a footprint having a 3-m (10-ft) diameter. Measurements were made within the original fenced area. Data have been plotted to show the vehicle path across the site. Spatial resolution is considerably better than that of the unaveraged aerial survey data. Ground-based data, when available, will offer improved spatial resolution. Aerial survey data are preferred when access is limited (over populated areas such as Pocatello, Idaho) and when large sites must be examined (as in the Trinity site discussed in the following section).

5.4 Trinity Site, New Mexico

Trinity, the first nuclear explosion, was detonated on July 16, 1945. The survey area, now part of the White Sands Missile Range, is sparsely populated and consists mostly of desert and mountains. Radioactive fallout and debris from this test were resurveyed using a fixed-wing aircraft in 1992.[18] An aerial radiological survey was the only practical means to investigate this area due to the rugged terrain and large area to be examined: 1,216 sq mi (3150 sq km).

Two man-made radionuclides were detected in the Trinity survey: an activation product, europium-152 (^{152}Eu), was seen around the original "ground zero"; a fission product, ^{137}Cs, was found throughout the area. The ^{137}Cs net count rate was extracted from the data and corrected for altitude variations:

$$Rate_{Cs\text{-}137} = (A - k \cdot B)\ e^{-\lambda_c(altitude\ -\ 91)}$$

where

A = spectral counts in the photopeak window (554–770 keV)
K = ratio of the photopeak window sum (A) to background window sum (B) away from the contaminated area
B = count rate in the background window (770–1370 keV)
λ_c = altitude dependence
altitude = altitude above the ground as determined by a radar altimeter

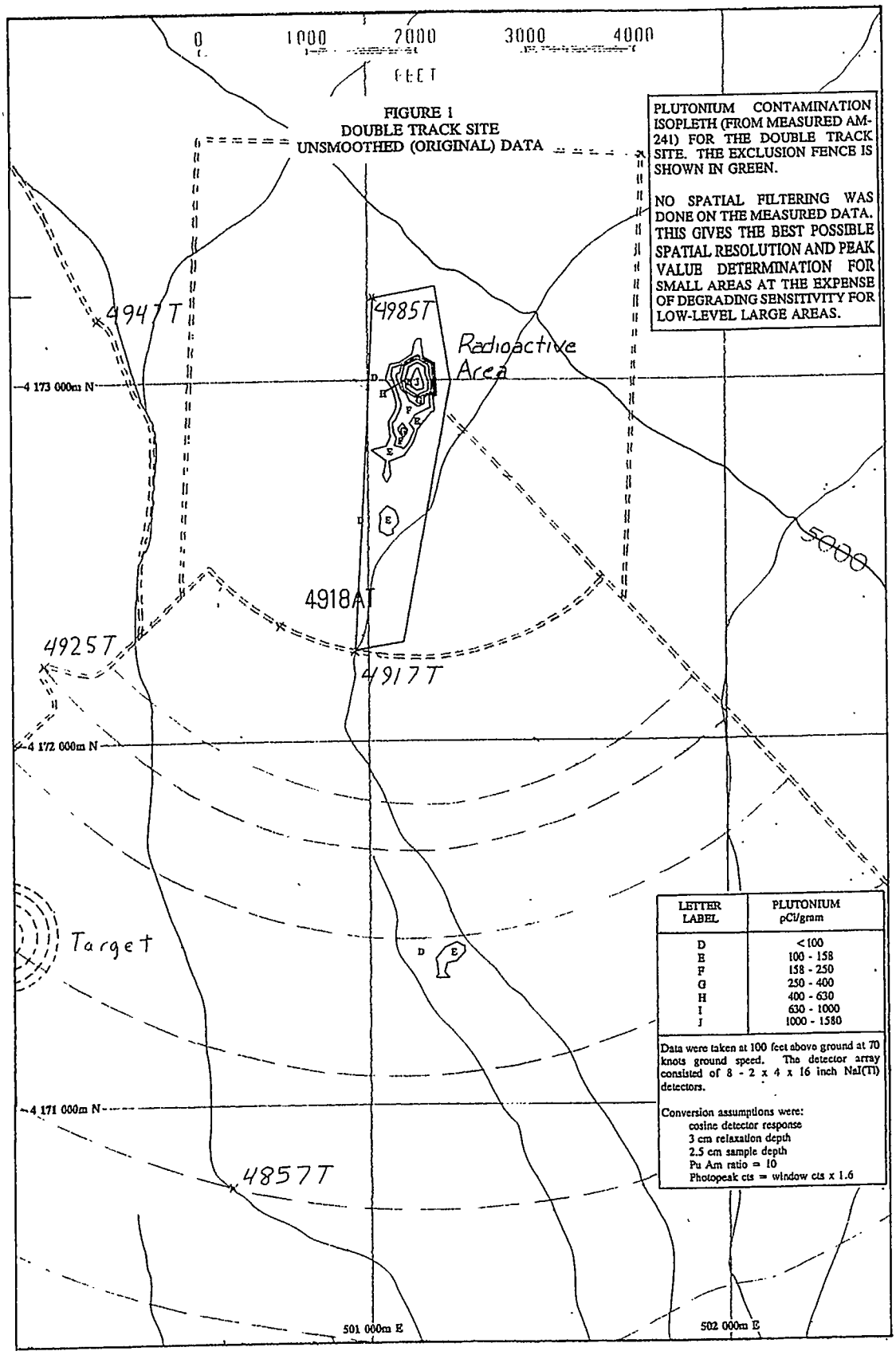

FIGURE 14. *DOUBLE TRACKS—ORIGINAL DATA*

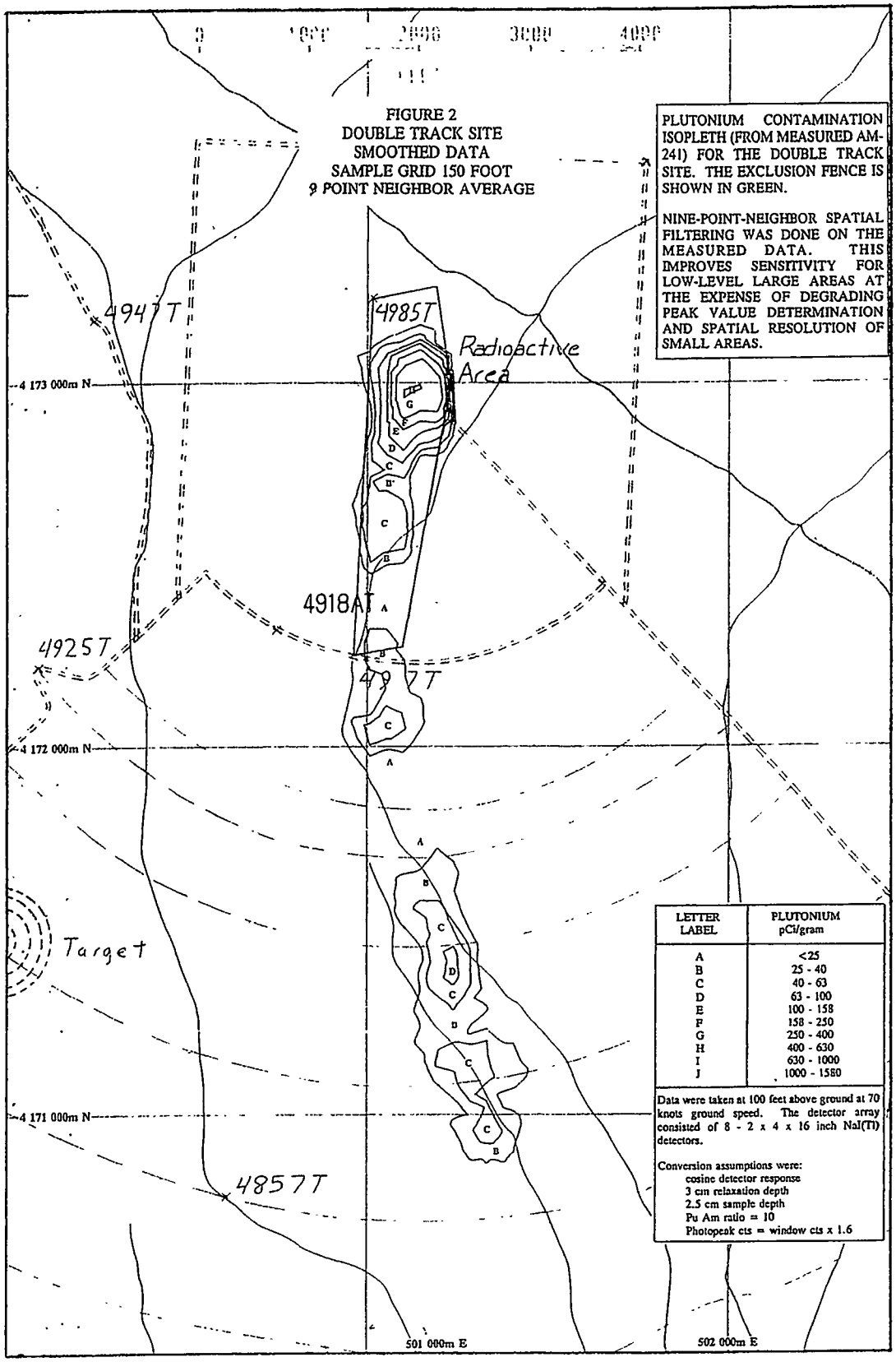

FIGURE 15. *DOUBLE TRACKS—AVERAGED DATA*

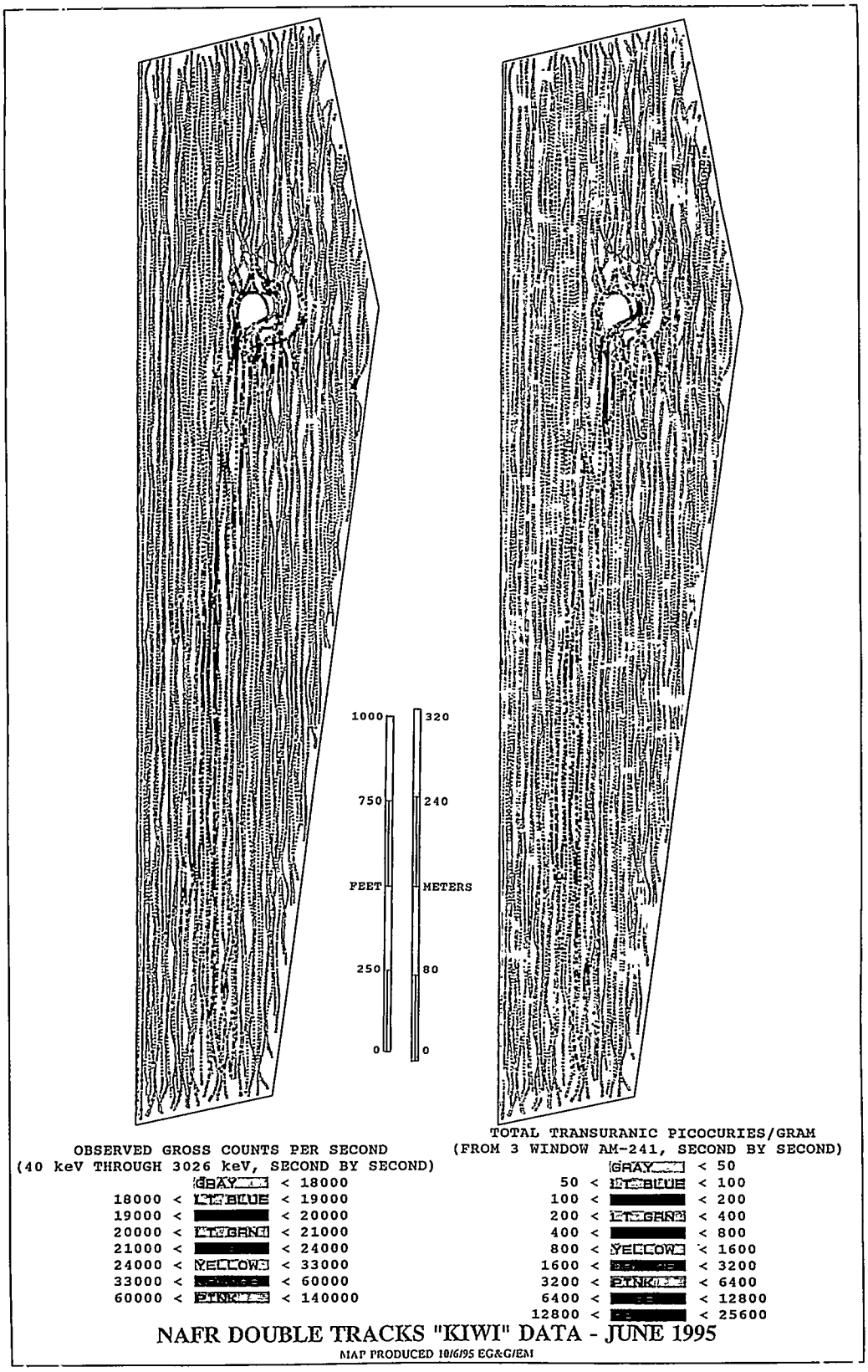

FIGURE 16. *DOUBLE TRACKS—GROUND-BASED SURVEY*

A map of ^{137}Cs contamination over the Trinity site is shown in Figure 17. Extensive contamination is evident almost half a century after the detonation. Data have been averaged in 5,000-ft squares over the survey area. The minimum detectable activity is 15 cps of ^{137}Cs, which corresponds to depositions of 0.03 $\mu Ci/m^2$ or 0.36 pCi/g.

5.5 El Paso/Juarez ^{60}Co Incident

The El Paso/Juarez survey was performed in support of a remediation project to clean up contamination dispersed when a medical irradiation source containing ^{60}Co was destroyed during destruction of the irradiation machine for scrap metal. Pellets containing ^{60}Co were spread throughout Juarez, Mexico, and El Paso, Texas. Pellets remaining with the irradiation source were melted with scrap steel. The contaminated steel was later fabricated into reinforcement bar for concrete construction.

Initially, contaminated materials were identified using conventional health physics instrumentation. This effort succeeded in locating much of the remains of the irradiation source and newly contaminated material. The radioactive material was removed from the areas as it was found.

An aerial radiation survey was carried out after the initial survey and clean-up operations to determine if any detectable contamination remained. Numerous millicurie-size point sources were located during the aerial survey. Source locations, activities, and identifications are shown in Figure 18. This map indicates that much of the material was missed during the initial survey and clean-up effort, illustrating the advantages of using aerial survey methods in areas that are difficult to examine from the ground.

5.6 Measurements of ^{16}N at the Pilgrim Station Nuclear Power Plant

Analysis of 1995 aerial survey data from the Pilgrim Station revealed substantial measurable activity at energies above 4 MeV in spectra acquired near the plant site. These detected high-energy gammas were attributed to the emission from ^{16}N that is produced during operation of the plant's boiling-water reactor. High-energy activity was detectable from 2,000 – 3,000 ft (600 – 1000 m) from the plant site; measurable levels spanned four orders of magnitude above the minimum detectable activity. Figure 19 shows a map of detectable ^{16}N activity.[19]

Due to the large area where ^{16}N activity could be detected, it was believed that the source could be either concentrated near the reactor building or dispersed around the plant site. Monte Carlo calculations were used to predict expected contour maps at various energies for both point and dispersed sources.[20] The "point source" was a half cylinder, 30 ft in diameter by 50 ft long; the "dispersed" source was a large square, 7,500 × 7,500 ft (2500 × 2500 m). A realistically sized airborne NaI(T*l*) detector was included in the model calculations. Results for 50-keV and 6-MeV source models are shown in Figure 20. The range of detectable activity from the point-source model is very energy-dependent, but the shape of the detected activity follows an approximate exponential decline from directly over the source for the range of energies studied. Detectable activity based on

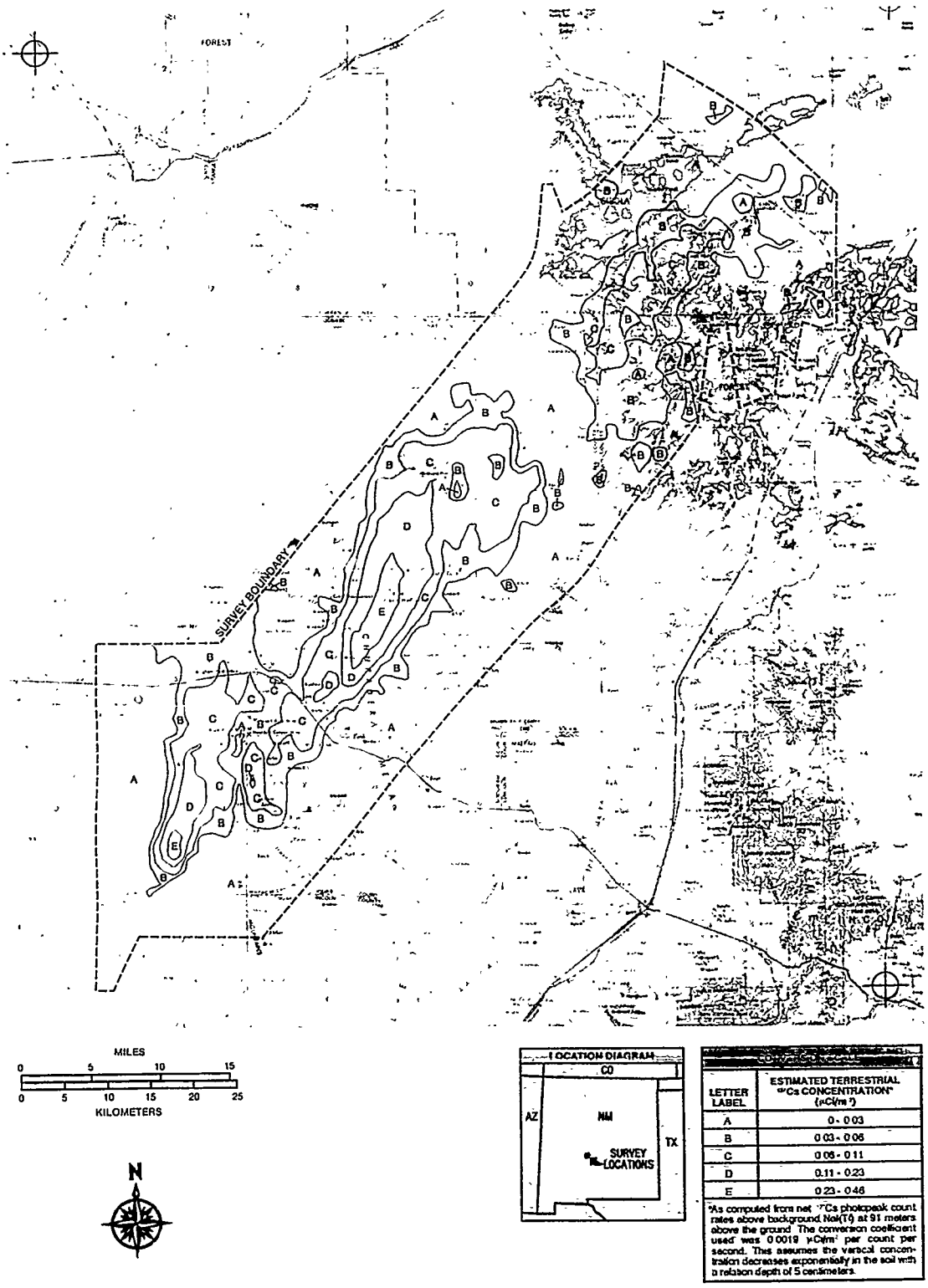

FIGURE 17. *TRINITY SITE—^{137}Cs*

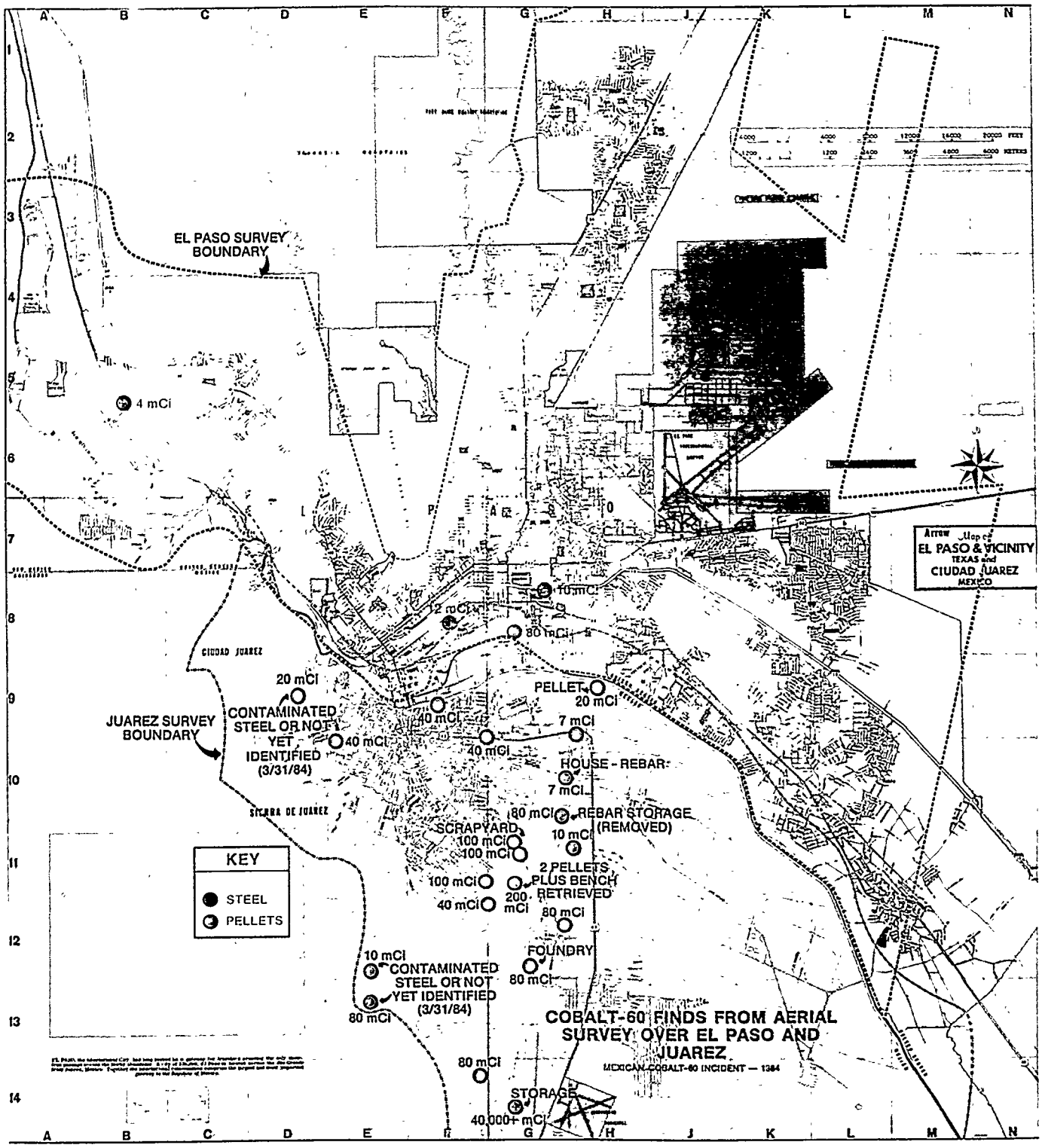

FIGURE 18. *EL PASO/JUAREZ—^{60}Co PELLETS FOUND DURING SURVEY*

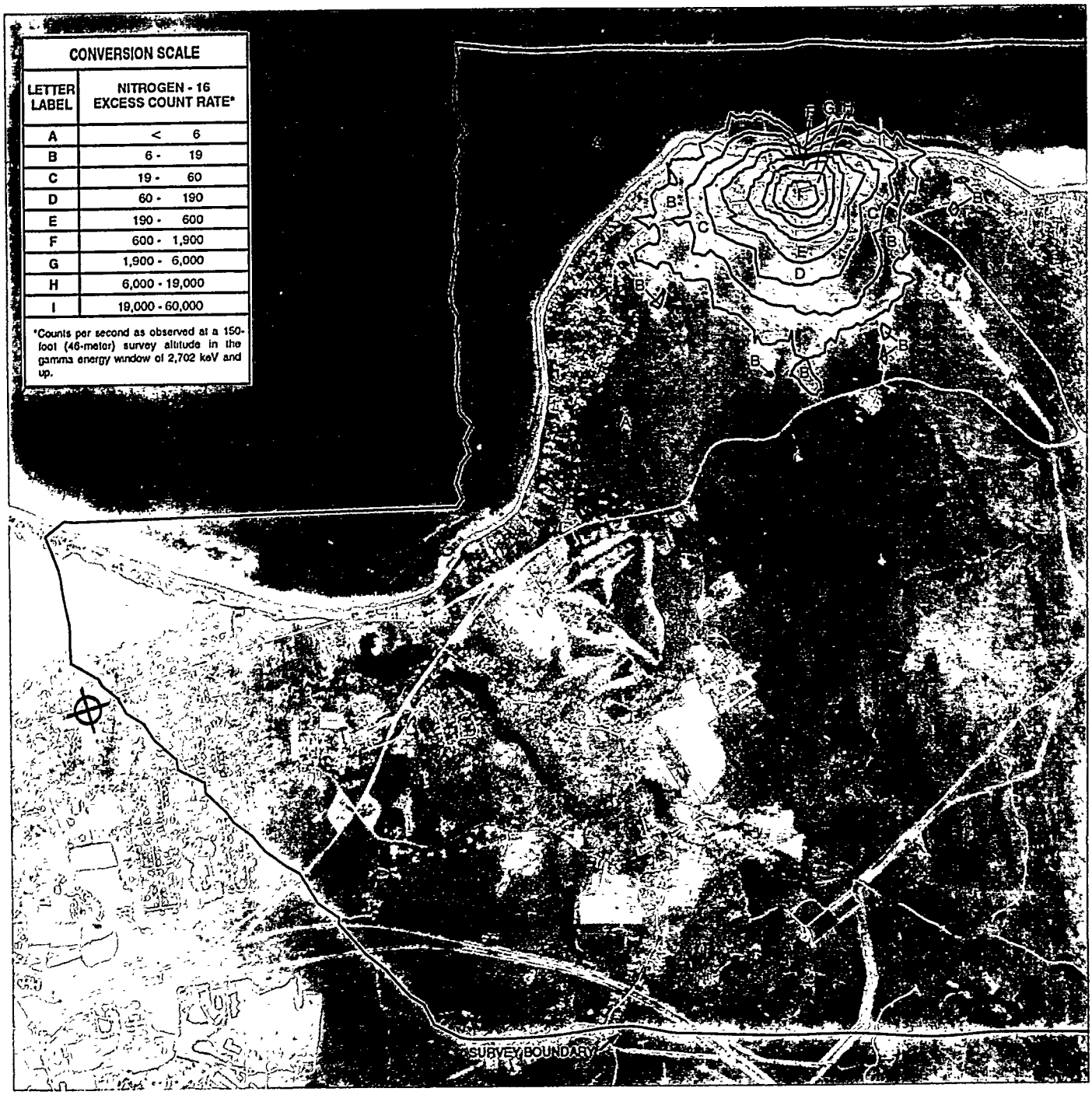

FIGURE 19. *MAP OF ^{16}N ACTIVITY AT PILGRIM STATION*

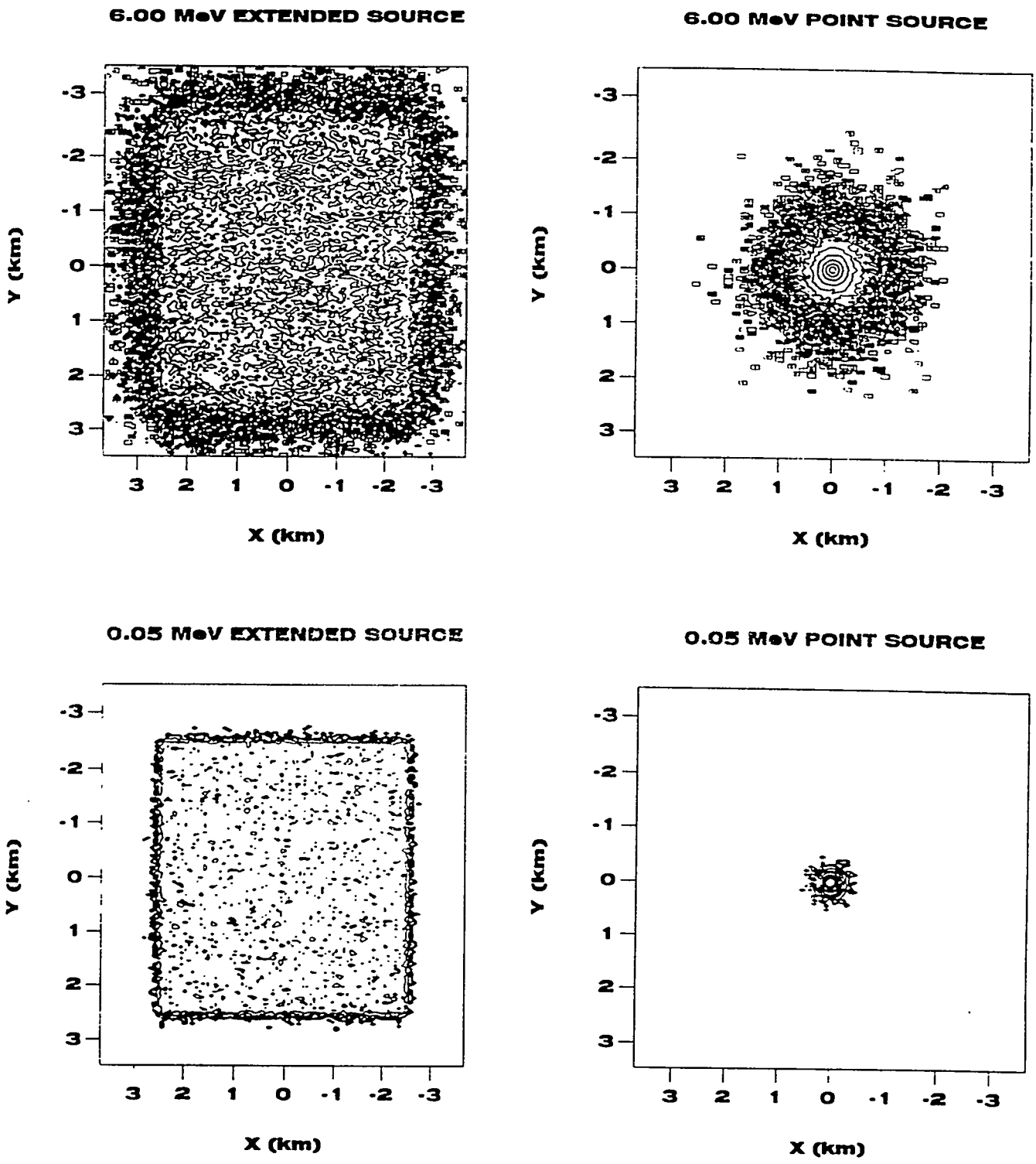

FIGURE 20. *MAPS OF DETECTED ACTIVITY BASED ON MONTE CARLO MODELING OF DISPERSED AND POINT SOURCES*

a dispersed source model is constant within the plume, with a relatively rapid decline at the plume boundary. Based on these model calculations, the Pilgrim Station ^{16}N map data are consistent with an intense, contained ^{16}N source at the plant site.

6.0 CONCLUSIONS

Aerial radiological surveys are a practical means to map contamination over areas that are large and/or difficult to access. Data represent an average of the area; achieving a similar coverage would require thousands of ground-based measurements. Individual sampling of an area cannot provide total coverage. Aerial survey methodology has been successful at hundreds of sites, in both routine and emergency response applications. Aerial survey methods compare favorably with other applicable techniques.

- ***Precision***

The precision of aerial survey measurements is very good. Results are reproducible; valid year-to-year comparisons of contamination are routinely performed. Typically measured exposure rates will vary only 2 percent from one survey to the next.

- ***Accuracy***

Exposure rates are accurate to within 15 percent or better; accuracy of isotopic results is better. Accuracy is limited by assumptions concerning deposition for radionuclide concentrations. Positional accuracy is ±3 m, limited by GPS differential technology.

- ***Spatial Representation***

Mapped radiation isopleths accurately reflect widely dispersed sources; isopleth maps of "point" sources are influenced by the relatively large detector "footprint."

- ***Completeness***

Aerial measuring methods are used to examine large areas better than any practical sampling technique.

- ***Comparability***

Aerial survey results compare well with laboratory soil sample counting and ground-based field measurements. Intercomparisons are ongoing.

▸ ***Sensitivity***

The sensitivity of aerial detection systems varies greatly depending on the radionuclide of interest (which is also true of all gamma spectroscopic measurements). Sensitivity is clearly less as compared with ground-based measurements but better than most Protective Action Guidelines.

▸ ***Limitations***

Weather and daylight restrictions limit aircraft operations.

ACKNOWLEDGMENTS

This work was performed for the U.S. Department of Energy by Bechtel Nevada under Contract No. DE-AC08-96NV11718.

REFERENCES

1. Jobst, J.E. Recent Advances in Airborne Radiometric Technology," *Remote Sensing Technology, Proceedings of a Symposium on Remote Sensing Technology in Support of the United States Department of Energy, 23-25 February 1983.* EGG-10282-1057, 1985; EG&G/EM, Las Vegas, Nevada.

2. Burson, Z.G.; Boyns, P.K.; Fritsche, A.E. "Technical Procedures for Characterizing the Terrestrial Gamma Radiation Environment By Aerial Surveys," *The Second Symposium on the Natural Radiation Environment, Houston, Texas, August 7-11, 1972.* EGG-1183-1559 (CONF-720805-8); 1972.

3. Belian, J.; Dayton, R. *NaI(Tl) Scintillation Detectors*. Bicron Corporation.

4. *Radiation, Environmental Data Acquisition, and Recorder System (REDAR IV) Manual.* 1981; Aerial Measurements Operations, EG&G, Las Vegas, Nevada.

5. Stampfl, A.; Riley, J.; Leckey, R. "Smoothing and Differentiation of Two-Dimensional Data." *Nuclear Instruments and Methods*, B16:427-433; 1986.

6. Lindeken, C.L.; Peterson, K.R.; Jones, D.E.; McMillen, R.E. "Geographical Variations in Environmental Radiation in the United States," *Proceedings of the Second International Symposium on the Natural Radiation Environment, August 7-11, 1972.* pp 317-33. Houston, Texas.

7. Claimant Jr., A.A.; Miller, C.B.; Minx, R.R.; Schlein, B. *Estimates of Ionizing Radiation Doses in the United States, 1960-2000.* U.S. EPA Report ORP/CSD72-1, 1972; EPA, Washington, D.C.

8. Proctor, A.E. [Private communication with M. F. Mohar, Washington Aerial Measurements Organization, Andrews Air Force Base]. October 1995.

9. Mohr, R.A. *Ground Truth Measurements at the Calvert County, Maryland Test Line.* Report No. EGG-10282-2066, 1985; EG&G/EM, Santa Barbara , California.

10. Proctor, A.E. [Private communication with G.D. Baker, Niagara Mohawk Power Corporation]. January 1997.

11. Hilton, L.K. "An Aerial Radiological Survey of the Rancho Seco Nuclear Generating Station." Report EGG-1183-1761, 1981; EG&G/EM, Las Vegas, Nevada.

12. Feimster, E.L. "An Aerial Radiological Survey of the Creeks and Tributaries near the Rancho Seco Nuclear Generating Station." Report EGG-10282-1086 (1986) EG&G/EM, Las Vegas, Nevada.

13. Boyns, P.K. "An Aerial Radiological Survey of the United States Department of Energy's Rocky Flats Plant and Surrounding Area." Report EGG-10617-1044, 1990; EG&G/EM, Las Vegas, Nevada.

14. Berry, H.A. "An Aerial Radiological Survey of Pocatello and Soda Springs, Idaho, and Surrounding Areas." Report EPA-8613, 1987; NTIS, Springfield, Virginia.

15. Proctor, A.E.; Hendricks, T.J. "An Aerial Radiological Survey of the Double Tracks Site and Surrounding Area." Report EGG-11265-1086, 1994; EG&G/EM, Las Vegas, Nevada.

16. Riedhauser, S.R.; Tipton, W.J. "In Situ Radiological Surveying at the Double Tracks Site." Report No. DOE/NV/11718-013, 1996; Bechtel Nevada, Las Vegas, Nevada.

17. Hendricks, T.J. "An Aerial Radiological Survey of the Double Track Site and Surrounding Area." Report EGG 11265-1466, 1995; EG&G/EM, Las Vegas, Nevada.

18. Fritzsche, A.E. "An Aerial Radiological Survey of the Trinity Fallout Area." Report EGG-11265-1037, 1994; EG&G/EM, Las Vegas, Nevada.

19. Proctor, A.E. *An Aerial Radiological Survey of the Pilgrim Station Nuclear Power Plant and Surrounding Area.* Report No. DOE/NV/11718-023, 1997; Bechtel Nevada, Las Vegas, Nevada.

20. Tunnell, L. [Letter to A. E. Proctor, Bechtel Nevada, regarding Monte Carlo modeling results]. January 29, 1997.

APPENDIX A

CONVERSION FACTOR AND MINIMUM DETECTABLE ACTIVITY DERIVATION

Conversion factors relate observed photopeak count rates to gamma-emitter activity on the ground. This appendix describes the derivation of these factors and their use in estimating minimum detectable activities. The estimates are used in calculating ground deposition for specific radionuclides from aerial survey data.

DETECTOR RESPONSE

Calculations are based on the concept of a detector "effective area," a value related to the physical size of the detector and the detector's energy-dependent response to gamma radiation. Effective areas for gamma rays of arbitrary energies at normal incidence to the helicopter-mounted detector pods are computed by interpolation, based on A. E. Fritsche's empirically determined relationships between effective areas versus gamma-ray energy and angle of incidence using the NaI(T*l*) detector pods.[1] A cubic interpolation of the logarithm of the effective area versus logarithm of energy was used based on an interpolating method that is known to produce well-behaved results.[2,3]

Detector angular response is approximated by a combined cosine and isotropic response:

$$R_\theta = [\ 1.0 + \mathit{cosine}\ (\theta)\ ] / 2.0$$

where θ is the angle of incidence of the detected gamma rays relative to an axis perpendicular to the face of the detector pod. The estimated effective area is the product of the interpolated energy response and the assumed angular response:

$$\mathit{Effective\ \ Area} = \mathit{Effective\ \ Area}_{\mathit{Energy},\ \theta\ .\ 0} \cdot R_\theta$$

CONVERSION FACTORS

Most sources of interest in aerial surveys are dispersed over large areas. The count rate due to a large source dispersed below the ground is found by integration as shown in Figure A-1:

$$C = \int_0^{\infty}\int_0^{\infty} \frac{S(z)\ A(E)\ R(\theta)}{4\ \pi\ d^2} e^{-\left(\frac{\mu}{\rho}\right)_a \rho_a r_a} e^{-\left(\frac{\mu}{\rho}\right)_s \rho_s r_s} 2\pi\ r\ dr\ dz$$

where

C	=	photopeak count rate
$S(z)$	=	source activity per unit volume
$A(E)$	=	detector effective area at energy, E (previously defined), for gamma rays at normal incidence ($\theta = 0$)
$R(\theta)$	=	the detector angular response
$d + d_a + d_s$	=	the distance between the source element and the detector
$(\mu/\rho)_a$, $(\mu/\rho)_s$	=	mass attenuation for air and soil, respectively
ρ_a, ρ_s	=	density of air and soil, respectively

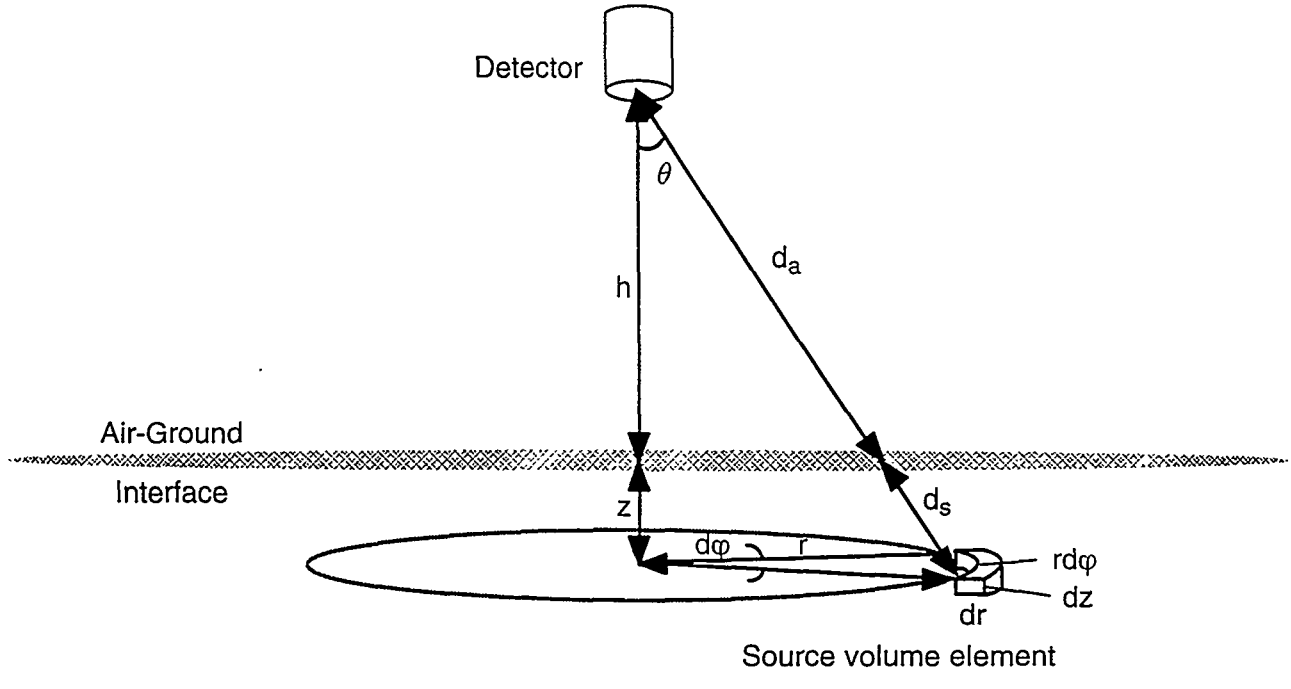

FIGURE A-1. ***GEOMETRY FOR RADIATION MEASUREMENTS.*** *The detector–soil elemental geometry applies to both aerial and in situ measurements. The count rate of the detector results from the integrated gamma-ray flux for all of the individual source elements.*

MINIMUM DETECTABLE ACTIVITY

Minimum detectable count rates are found by calculating L_C (critical level) and L_D (detection limit) values for a typical two-window net count at a specific energy, using a realistic background spectrum. Two representative background spectra are used, one from a rural area in Calvert County, Maryland,[4] and a second from a desert area near Lake Mohave National Recreation Area, Nevada.[5] An uncertainty value for a two-window net photopeak area is assumed to be equal to the square root sum of the variances of counts into equal-sized photopeak windows. For purposes of this estimate, it is assumed that the photopeak window is the sum of the background from 10 percent below to 10 percent above the energy of the radionuclide photopeak under consideration:

$$Total\ \ Photopeak\ \ Rate = \sum_{i=j,E=0.9E_{peak}}^{k,E=1.1E_{peak}} C_i$$

C_i represents the counts in the ith spectrum channel for a one-second spectrum. (The representative spectrum used contains a background continuum and photopeaks from naturally occurring radionuclides.) In practice, the net photopeak rate would be calculated from the difference between the total photopeak rate and a normalized background count rate. (All aerial survey data are based on a one-second counting period.) For estimating purposes, the background count rate is assumed to be equal to the estimated photopeak rate, leading to an uncertainty for the net count rate:

$$\sigma_{Net\ Photopeak} = \sqrt{\sigma^2_{Total\ Photopeak} + \sigma^2_{Background}} = \sigma_{Total\ Photopeak}\sqrt{2}$$

A selected "confidence level" value is used in determining the minimum detectable count rate, L_D, based on the cumulative probability distribution, $P(x)$, using methods described in Appendix B and is expressed as follows:

$$Confidence\ \ Level = P(x)$$
$$L_c = x\ \sigma_{Total\ Photopeak}$$
$$L_d = 2\ L_c + x^2$$

Useful confidence levels are 0.95 (95 percent) $L_C = 1.65\sigma$; 0.99 (99 percent) $L_C = 2.33\sigma$; 0.995 (99.5 percent) $L_C = 2.58\sigma$; and 0.999 (99.9 percent) $L_C = 3.08\sigma$.

ESTIMATES FOR AERIAL SURVEY SOURCES

▸ Point-Source Flyover

The point-source flyover is of interest in determining whether a "lost" source can be found from the air. The El Paso/Juarez pellet search was a situation where small sources were located using aerial survey methods.

The count rate detected from a source of known strength is computed from the detector solid angle as a function of time. The detector is moving during the measurement, and the solid angle varies, as shown in Figure A-2. The total count seen in a one-second data interval is found by integration.

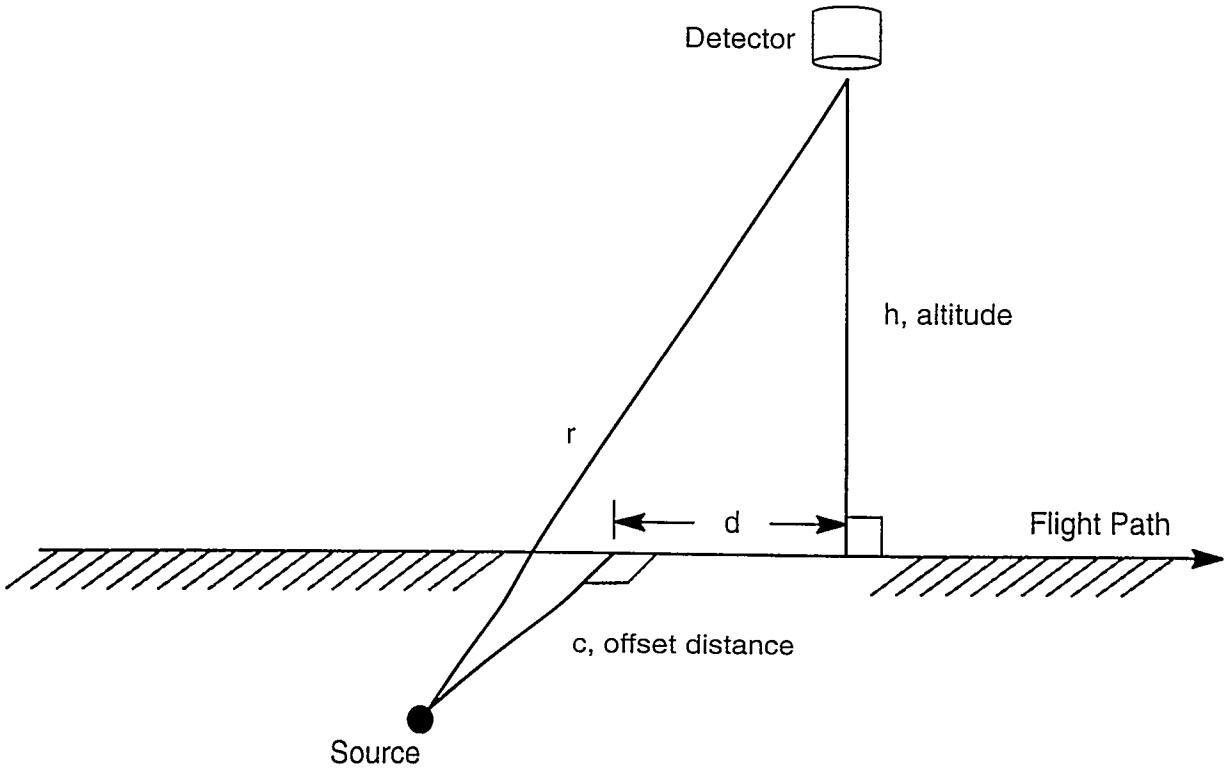

FIGURE A-2. *GEOMETRY FOR POINT-SOURCE FLYOVER*

The count rate due to an airborne detector from a ground-based point source can be expressed as follows:

$$Rate = A\ S\ /\ (4\ \pi\ r^2)$$

where

A = detector effective area
S = point source gamma emission, gammas-sec^{-1}
r = distance to the detector; $r=(h^2 + d^2 + c^2)^{1/2}$
h = the detector altitude above the ground (AGL)
c = the distance between the source and a projection of the flight line along the ground (offset distance)
d = the distance along the flight path; $d = v \cdot t$ (airspeed · time)

The detector angular response is assumed to be an average of isotropic and cosine responses. This can be expressed as follows:

$$R_\theta = \frac{(1 + cosine\ (\theta))}{2.0} = \frac{1}{2}\left(1 + \frac{h}{(h^2+c^2+v^2t^2)^{1/2}}\right)$$

Including the effect of air attenuation, the integrated count rate over the interval $(-t,t)$ is calculated as follows:

$$N = \frac{S\ A_e}{4\ \pi}\int_{-t}^{t} R_\theta \frac{e^{-\left(\frac{\mu}{\rho}\right)_a \rho_a\ (c^2+h^2+v^2t^2)^{1/2}}}{(c^2+h^2+v^2t^2)}\ dt$$

The required source strength is found by setting N equal to L_D and rearranging the previous equation to produce the following equation:

$$S = \frac{4\ \pi\ L_d}{A_e}\left(\int_{-t}^{t} R_\theta \frac{e^{-\left(\frac{\mu}{\rho}\right)_a \rho_a\ (c^2+h^2+v^2t^2)^{1/2}}}{(c^2+h^2+v^2t^2)}\ dt\right)^{-1}$$

▸ Distributed Sources—Uniform Surface Source

Nuclear accidents would be expected to deposit radioactive material over large areas. Since the aerial survey response occurs relatively soon after the deposition, very little percolation of radioactive material into the soil is expected.

The photopeak flux, observed at a distance h above the surface from a monoenergetic gamma emitter distributed uniformly on the surface, can be calculated as follows:

$$\phi = \frac{S}{4\pi}\int_0^{2\pi} d\theta \int_0^{\infty} \frac{e^{-\left(\frac{\mu}{\rho}\right)_a \rho_a\ d}}{d^2} r\ dr$$

where d is the distance from a source element on the surface, shown in Figure A-1 as d_a. Since the geometry is symmetrical in this cylindrical coordinate system, the first integration can be carried out:

$$\phi = \frac{S}{2}\int_0^{\infty} \frac{e^{-\left(\frac{\mu}{\rho}\right)_a \rho_a\ d}}{d^2} r\ dr$$

Changing variables:

r = h tangent (θ)
dr = h secant^2(θ) $d\theta$
h = d cosine (θ)
d = h secant (θ) where h is the distance between the detector and the surface

$$\phi = \frac{S}{2}\int_0^{\frac{\pi}{2}} \frac{e^{-\left(\frac{\mu}{\rho}\right)_a \rho_a h \sec(\theta)}}{h^2 \sec^2(\theta)} h \tan(\theta)\ h \sec^2(\theta)\ d\theta$$

Including the NaI(T*l*) detector-pod angular response as an effective area, $A = A_e \cdot R_\theta$, the count rate measured by the airborne pods is calculated as follows:

$$N = A \cdot \phi = \frac{A_e S}{2}\int_0^{\frac{\pi}{2}} R_\theta\ e^{-\left(\frac{\mu}{\rho}\right)_a \rho_a h \sec(\theta)} \tan(\theta)\ d\theta$$

The required source strength is found by setting N equal to L_D and rearranging the previous equation:

$$S = \frac{2L_d}{A_e}\left(\int_0^{\frac{\pi}{2}} R_\theta\ e^{-\left(\frac{\mu}{\rho}\right)_a \rho_a h \sec(\theta)} \tan(\theta)\ d\theta\right)^{-1}$$

▸ Distributed Sources—Source Uniformly Distributed in the Soil

Naturally occurring radioactive material, such as uranium mine tailings, is assumed to be uniformly radioactive to depths where the material contributes minimally to the detected count rate. Calculation of uniformly and exponentially distributed sources is based on NCRP 50[6] and Tipton, et al.[7] The modified detector response used above is included here also. In the cylindrical coordinate system of (x,z,θ), the following equation applies:

$$\phi = \frac{S}{4\pi}\int_0^{2\pi} d\theta \int_0^{\infty} dz \int_0^{\infty} \frac{e^{-\left(\frac{\mu}{\rho}\right)_a \rho_a r_a}\ e^{-\left(\frac{\mu}{\rho}\right)_s \rho_s r_s}}{r^2}\ x\ dx$$

where

ϕ	=	photopeak flux at the detector
S	=	activity per unit volume; [(γ/s)/cm^3]
r	=	detector-to-source distance in the air and the soil combined $r = r_a + r_s$
$(\mu/r)_a, (\mu/r)_s$	=	air and soil mass attenuation coefficients for the monoenergetic gamma energy; (cm^2/g)
ρ_a, ρ_s	=	air and soil density (g/cm^3)

The previous equation may be integrated over θ to yield the following equation:

$$\phi = \frac{S}{2} \int_0^{\infty} dz \int_0^{\infty} \frac{e^{-\left(\frac{\mu}{\rho}\right)_a \rho_a r_a} \; e^{-\left(\frac{\mu}{\rho}\right)_s \rho_s r_s}}{r^2} \; x \; dx$$

Changing variables:

$(h+z)$	=	r cosine (θ)
h	=	r_a cosine (θ)
z	=	r_s cosine (θ)
r	=	$(h+z)$secant (θ)
r_a	=	h secant (θ)
r_s	=	x secant (θ)
x	=	$(h+z)$ tangent (θ)
dx	=	$(h+z)$ secant^2 (θ) $d\theta$

$$\phi = \frac{S}{2} \int_0^{\frac{\pi}{2}} d\theta \int_0^{\infty} \frac{e^{-\left(\frac{\mu}{\rho}\right)_a \rho_a h \sec(\theta)} \; e^{-\left(\frac{\mu}{\rho}\right)_s \rho_s z \sec(\theta)}}{(h+z)^2 \sec^2(\theta)} (h+z)\tan(\theta) \; (h+z)\sec^2(\theta) \; dz$$

Rearranging the variables and integrating the previous equation over z yields the following equation:

$$\phi = \frac{S}{2} \int_0^{\frac{\pi}{2}} \frac{\tan(\theta)\ e^{-\left(\frac{\mu}{\rho}\right)_a \rho_a h \sec(\theta)}}{\left(\frac{\mu}{\rho}\right)_s \rho_s \sec(\theta)}\ d\theta$$

The detected gamma count rate, N, is equal to the product of the flux and detector area. Including the energy and angle dependence of the effective area yields an equation for the net count rate at the detector:

$$N = A\,\phi = \frac{A_e\ S}{2} \int_0^{\frac{\pi}{2}} R_\theta \frac{\tan(\theta)\ e^{-\left(\frac{\mu}{\rho}\right)_a \rho_a h \sec(\theta)}}{\left(\frac{\mu}{\rho}\right)_s \rho_s \sec(\theta)}\ d\theta$$

Setting N equal to L_D, converting S from (γ-sec^{-1}-cm^{-3}) to (γ-sec^{-1}-g^{-1}), and rearranging the equation results in the following equation:

$$S = \frac{2L_d}{A_e \rho_s} \left(\int_0^{\frac{\pi}{2}} R_\theta \frac{\tan(\theta)\ e^{-\left(\frac{\mu}{\rho}\right)_a \rho_a h \sec(\theta)}}{\left(\frac{\mu}{\rho}\right)_s \rho_s \sec(\theta)}\ d\theta \right)^{-1}$$

Lastly, S may be converted from (γ-sec^{-1}-g^{-1}) to (*disintegration*-sec^{-1}-g^{-1}) by dividing by the branching ratio.

▸ Distributed Sources—Source Exponentially Distributed in the Soil

Exponentially distributed radioactive material is assumed to have a "classic" deposition pattern. Exponentially distributed material is assumed for materials initially deposited on the surface that have had an opportunity to seep into the surrounding soil.

This case differs from the previous one in that the radionuclide concentration in the soil, S, is a function of the soil depth below the surface, z. An exponential dependence of activity versus depth is assumed:

$$S = S_0 e^{-\alpha z}$$

where S_0 is the radionuclide concentration at $z = 0$ and α is a constant. The gamma flux arriving at the detector can be expressed as follows:

$$\phi = \frac{S_0}{2} \int_0^{\frac{\pi}{2}} d\theta \int_0^{\infty} \frac{e^{-\left(\frac{\mu}{\rho}\right)_a \rho_a h \sec(\theta)} \; e^{-\left(\left(\frac{\mu}{\rho}\right)_s \rho_s z \sec(\theta) + \alpha z\right)}}{(h+z)^2 \sec^2(\theta)} (h+z)^2 \tan(\theta) \sec^2(\theta) \, dz$$

Rearranging the variables and integrating the previous equation over z yields the following equation:

$$\phi = \frac{S_0}{2} \int_0^{\frac{\pi}{2}} \frac{\tan(\theta) \; e^{-\left(\frac{\mu}{\rho}\right)_a \rho_a h \sec(\theta)}}{\alpha + \left(\frac{\mu}{\rho}\right)_s \rho_s \sec(\theta)} \, d\theta$$

The detected gamma count rate, N, is equal to the product of the flux and detector area. Including the effective area in the flux equation yields an expression for the detected count rate:

$$N = A \, \phi = \frac{A_e S_0}{2} \int_0^{\frac{\pi}{2}} R_\theta \frac{\tan(\theta) \; e^{-\left(\frac{\mu}{\rho}\right)_a \rho_a h \sec(\theta)}}{\alpha + \left(\frac{\mu}{\rho}\right)_s \rho_s \sec(\theta)} \, d\theta$$

It is often useful to compare the count rates measured by the aerial detection system to those determined by soil sample collection and counting. Since the collection of soil samples requires that a finite depth of soil be removed and mixed prior to counting, the count rates determined during soil sampling and counting are based on averaged contamination levels over some sampling depth, "z." The surface contamination, S_0, used in the previous equation is related to an averaged contamination as follows:

$$S_z = \frac{1}{z}\int_0^z S_0 e^{-(\alpha y)} dy = \frac{S_0}{\alpha z}(1 - e^{-\alpha z})$$

$$S_0 = S_z \frac{\alpha z}{(1 - e^{-\alpha z})}$$

Substituting an average radionuclide concentration, S_z, in the first "z" of soil depth for S_0 in the count rate integral yields the following equation:

$$N = A\,\phi = \frac{A_e S_z}{2} \frac{\alpha z}{(1 - e^{-\alpha z})} \int_0^{\frac{\pi}{2}} R_\theta \frac{\tan(\theta)\; e^{-\left(\frac{\mu}{\rho}\right)_a \rho_a h \sec(\theta)}}{\alpha + \left(\frac{\mu}{\rho}\right)_s \rho_s \sec(\theta)} d\theta$$

Setting N equal to L_D, converting S_z from (γ-cm^{-3}) to (γ-g^{-1}), and rearranging the previous equation results in an equation for the averaged contamination at a minimum detectable depth averaged contamination:

$$S_z = \frac{2L_d}{A_e \rho_s} \frac{(1 - e^{-\alpha z})}{\alpha z} \left(\int_0^{\frac{\pi}{2}} R_\theta \frac{\tan(\theta)\; e^{-\left(\frac{\mu}{\rho}\right)_a \rho_a h \sec(\theta)}}{\alpha + \left(\frac{\mu}{\rho}\right)_s \rho_s \sec(\theta)} d\theta \right)^{-1}$$

Lastly, S_z may be converted from (γ-sec^{-1}-g^{-1}) to (*disintegration*-sec^{-1}-g^{-1}) by dividing by the branching ratio.

REFERENCES

1. Fritsche, A.E. [Letter to the Nuclear Radiation Department personnel, Remote Sensing Laboratory, regarding "NaI Pod Effective Areas," NRD-89-066]. March 1, 1989.

2. Akima, H. "A New Method of Interpolation and Smooth Curve Fitting Based on Local Procedures." *J. Assoc. for Computing Mach.,* 17:4:589–602; October 1970.

3. Akima, H. "Algorithm 433, Interpolation and Smooth Curve Fitting Based on Local Procedures (E2)." In: Collected Algorithms from CACM. New York: Association for Computing Machinery; 1978:433-P 1.

4. Proctor, A.E. [Oral communication with R. Maurer]. October 1996.

5. Proctor, A.E. [Oral communication with D.P. Colton]. October 1996.

6. *Environmental Radiation Measurements.* NCRP Report 50, National Council on Radiation Protection and Measurements, 1977; pp 32-35. Washington, D.C.

7. J. Tipton, et. al. *An In Situ Determination of ^{241}Am on Enewetak Atoll.* Report No. EGG-1183-1778, 1981; EG&G Energy Measurements Group, Las Vegas, Nevada.

APPENDIX B

DETECTION LIMITS

The results of an aerial radiological survey provide information about radiation levels at nuclear power plant sites (generally above background) and in the surrounding areas (generally a relatively constant background). Higher levels of radiation within the plant site are expected; the plant operator usually has ground-based measurements of the site. Aerial radiological survey data provide a check on the extent of higher levels of radiation near the site. Due to the large survey footprint, aerial data are only an approximate measure of the extent of site-based radioactivity. There are less costly means than aerial radiological surveys to determine that the exposure rate (ground-based radioactivity, etc.) within the site boundary of a nuclear power plant is greater than the exposure rate of the surrounding area.

Radioactivity in the off-site area surrounding the plant, especially from plant site emissions, is assumed to consist of large areas (compared to the survey detection footprint) of natural and man-made radioactivity. Activity outside the boundary of the plant site will likely be due to naturally occurring radionuclides only. Detection limits used in analyzing survey data are established to identify the lowest practical off-site contamination levels.

Aerial radiological survey data consist of many single measurements distributed over the survey area. It has been found from previous surveys that the survey data always contain large regions of background radiation with a few anomalous locations (*i.e.*, the reactor site). Knowing this and excluding the plant site, the survey data can be treated as a single, large data set for isotopic net counts and man-made gross count rate (MMGC). A typical nuclear power plant survey, for example, the Nine Mile Point/James FitzPatrick survey,[1] a half-circle area having a radius of 2.5 mi, contains approximately 40,000 observations, a population sufficiently large that statistical analysis can be applied. Detection limits, minimum detectable activities (MDAs), can be estimated using methods similar to those developed by Currie.[2] The following discussion can be applied to both MMGC and isotopic net count rates.

Currie defines two limits that are useful in analyzing survey data: (a) a critical level which is the minimum count rate where one would assume that data from a footprint are different from the background in the survey area and (b) a detection limit which is the minimum activity source that can reliably be detected. The critical level, L_C, is determined by considering the distribution of count rates in the background data set (generally the survey area outside the immediate reactor site) so that a fraction of all measured (calculated) quantities in the background data are less than or equal to L_C. This level addresses "type 1 errors" (failures to detect anomalous data). If a measurement or group of measurements is above L_C, then this region of the survey requires further examination. L_C is defined in the following expression:

$$L_C = k \cdot \sigma$$

The value of σ is determined from the distribution of the survey data. The value of k is selected based on the integral of a normal distribution from minus infinity to L_C such that a desired fraction (*e.g.*, 99.9 percent) of the observations in the distribution of background data is less than L_C, assuming normally distributed data. The desired fraction (or percentage) of the cumulative distribution of observations is commonly referred to as the *confidence level*. Examination of actual distributions of survey data supports this assumption. A measured value exceeding L_C would be assumed to indicate radiation above background within a specified confidence level.

L_C should not be considered a dimensioned quantity. Individually measured and/or computed values would be distributed around the "real" value (mean value). A single, measured observation equal to L_C could arise from measuring a range of "actual" activity levels.

The detection limit, L_D, may be understood by considering a single measurement of one survey footprint. Multiple measurements of this footprint would yield a distribution of values with a centroid corresponding to the actual (mean) activity within the footprint. Assuming a normal distribution of measurement values, Currie defines L_D as the minimum activity (centroid of the distribution of measurements) where a desired fraction of all single measurements will fall above L_C as expressed in the following equation:

$$L_D = 2\ L_C + k^2$$

This equation is based on Currie's analysis for radiation-counting data (Poisson statistics). For example, assuming a value of k corresponding to a 99.9 percent confidence level, greater than 99.9 percent of all measured and/or calculated values for any "detectable" source (whose activity is L_D or greater) will be above L_C. This ensures that a source whose activity is equal to or greater than L_D will "always" be detected. L_D represents the lowest-activity level that the survey detection process will consistently find.

The lowest-radiation isopleth level in a typical contour plot would be set at (or near) L_C while L_D would be the stated MDA. (Higher contours are customarily defined in terms of "levels per decade," leading to an approximate logarithmic scale.) Radionuclide activities determined from net count values that are greater than L_C but less than L_D are reported although they are below the "detection limit" of the instrumentation.

Figure B-1 shows the distribution of MMGC values from the survey of the Nine Mile Point/James FitzPatrick Nuclear Power Plants, after applying sliding interval averaging.[1] This distribution deviates from a true normal distribution, but a usable uncertainty equal to 256 (σ = 256) was calculated assuming a normal distribution. Isotopic net count rates of ^{137}Cs, ^{16}N, and ^{60}Co were

distributed around zero but have different uncertainty values. These statistical uncertainties and corresponding MDAs are listed in Table B-1.

The previous analysis provides a rigorous means to estimate critical levels and MDAs for survey data analysis. Unfortunately, application of statistical techniques leads to a problem of outliers. For example, basing L_C on a 99.5 percent confidence level will ensure that 99.5 percent of measurements from background areas (assumed to be free of man-made radiation) will fall below L_C, and 0.5 percent of all background-area data will be above L_C, leading to an erroneous conclusion that 0.5 percent of the total survey area is contaminated. For a set of 40,000 observations, 0.5 percent represents 200 survey footprint measurements.

Setting L_C at a value well above the background distribution but below the highest level seen over the nuclear power plant site eliminates the outlier problem. This approach has been used in the past, but the resulting large increase in MDA fails to detect low-level contamination. Another method deals with outliers by requiring spatial correlations between data of minimal activity. Here it is assumed that individually measured values near L_C are outliers if the data nearest the value in question are below L_C. Data values much higher than L_C do not require spatial correlations to be valid.

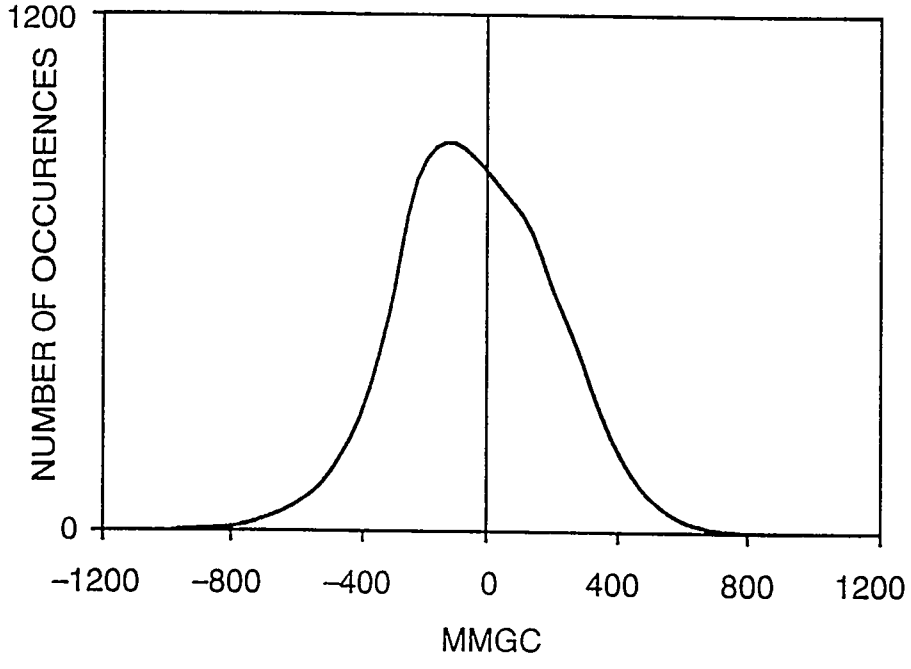

FIGURE B-1. *DISTRIBUTION OF MAN-MADE RADIATION DATA*

Table B-1. Empirically Determined Detection Limits for the Nine Mile Point/ James FitzPatrick Survey

Radionuclide	Total Uncertainty ($\sigma_{survey\ data}$)	Critical Level (L_C)		Detection Limit (L_D)	
		99.5% Confidence Level [a]	99.9% Confidence Level	99.5% Confidence Level	99.9% Confidence Level
MMGC	256	658 net cps	794 net cps	1322 net cps	1597 net cps
^{60}Co	9.56	25 net cps	30 net cps	0.027 μCi/m^2 0.27 pCi/g (u) [b] 0.64 pCi/g (e) [c]	0.032 μCi/m^2 0.32 pCi/g (u) 0.74 pCi/g (e)
^{16}N [d]	2.36	6.06 net cps	7.30 net cps	18 net cps	23 net cps
^{137}Cs	13.3	34 net cps	41 net cps	0.064 μCi/m^2 0.82 pCi/g (u) 1.6 pCi/g (e)	0.075 μCi/m^2 0.97 pCi/g (u) 1.9 pCi/g (e)

[a] Confidence level as defined in the text.
[b] A uniform distribution of radioactive material versus depth throughout the soil.
[c] An exponential distribution of radioactive material having a relaxation length of 3 cm was assumed. The stated value is an average over the first 2.5 cm.
[d] ^{16}N is assumed to be a point source. No conversion factor is available to relate net cps to concentration.

Radiation isopleth plots using L_C values based on 95, 99, 99.5 and 99.9 percent confidence levels are examined for spatial correlations. Confidence-level plots of 95 and 99 percent often contain many outliers. The 99.9 percent confidence level is customarily selected as the lowest-contour level in published isopleth plots. The likelihood of an outlier appearing in the plot is 0.001. This yields a relatively "clean" contour map. The probability that two adjacent data measured on two different flight lines are both outliers is $(0.001)^2 = 1 \times 10^{-6}$. Since adjacent data create contours on the map, the likelihood of presenting erroneous evidence of contamination is extremely small.

It is also possible to determine L_C and L_D from model calculations. Such calculations are useful in planning survey operations. Table B-2 shows estimated critical levels and MDA values for the usual helicopter survey conditions including a flight altitude of 46 m (150 ft), an airspeed of 70 knots, and the use of eight 2- × 4- × 16-in NaI(T*l*) detectors. These conditions are similar to those of the Nine Mile Point/James FitzPatrick survey. Net count rates and conversions from count rates to activities are computed using the modeling that is described in Appendix A. An estimated uncertainty is calculated for an energy region of an assumed background spectrum; L_C and L_D are calculated from the uncertainty values. These rates are converted to activities by integrating the expected contributions to the count rate for an assumed source, and deriving the activity from the fraction of gamma rays emitted by that source, which are counted at the detector.

Table B-2. CALCULATED CRITICAL LEVELS AND MINIMUM DETECTABLE ACTIVITY VERSUS ENERGY FOR ISOTOPIC ANALYSIS BASED ON A REALISTIC BACKGROUND SPECTRUM

Assuming: 70-knot airspeed, 150-ft survey altitude, 2.5-cm sample averaging depth, 3-cm relaxation depth, unity branching ratio, and unity spectral window factor, and 95 percent confidence level[a]

Energy (keV)	Net Spectral Window Count Rates		Minimum Detectable Activity (L_D)				
			Point Source		Distributed Source		
	Critical Level (L_C)	Minimum Detectable Activity (L_D)	Directly Beneath the Detector (mCi)	Beneath the Detector Offset by 150 ft (46 m) (mCi)	Uniform Distribution Versus Depth (pCi/g)	Exponential Distribution Versus Depth (pCi/g)	Uniformly Distributed on the Surface ($\mu Ci/m^2$)
60	36	75	0.30	1.10	2.44	1.66	0.11
200	46	95	0.20	0.70	1.12	0.76	0.05
600	36	74	0.10	0.30	0.55	0.38	0.025
1,500	23	48	0.10	0.30	0.50	0.34	0.022
2,000	16	34	0.10	0.30	0.51	0.34	0.023
3,000	6	14	0.10	0.40	0.48	0.33	0.022

[a] Confidence level as defined in the text.

REFERENCES

1. Proctor, A.E. *An Aerial Radiological Survey of the Nine Mile Point and James FitzPatrick Nuclear Power Plants and Surrounding Areas."* Report No. DOE/NV/11718-021, 1997; Bechtel Nevada, Las Vegas, Nevada.

2. Currie, L.A. "Limits for Quantitative Detection and Quantitative Determination; Applications to Radiochemistry." *Analytical Chemistry,* 40:3:586–593; 1968.